

ARMY
CERC 93-8

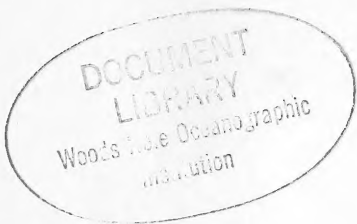
Technical Report CERC-93-8
May 1993



**US Army Corps
of Engineers**
Waterways Experiment
Station

Coastal Scour Problems and Methods for Prediction of Maximum Scour

by *Jimmy E. Fowler*
Coastal Engineering Research Center



Microfilm and microfiche editions of this report are available from the University Microfilms International, 300 North Zeeb Road, Ann Arbor, Michigan 48106.

Approved For Public Release; Distribution Is Unlimited

GB
450
.T45
no. CERC-
93-8

The contents of this report are not to be used for advertising, publication, or promotional purposes. Citation of trade names does not constitute an official endorsement or approval of the use of such commercial products.



Coastal Scour Problems and Methods for Prediction of Maximum Scour

by Jimmy E. Fowler
Coastal Engineering Research Center
U.S. Army Corps of Engineers
Waterways Experiment Station
3909 Halls Ferry Road
Vicksburg, MS 39180-6199

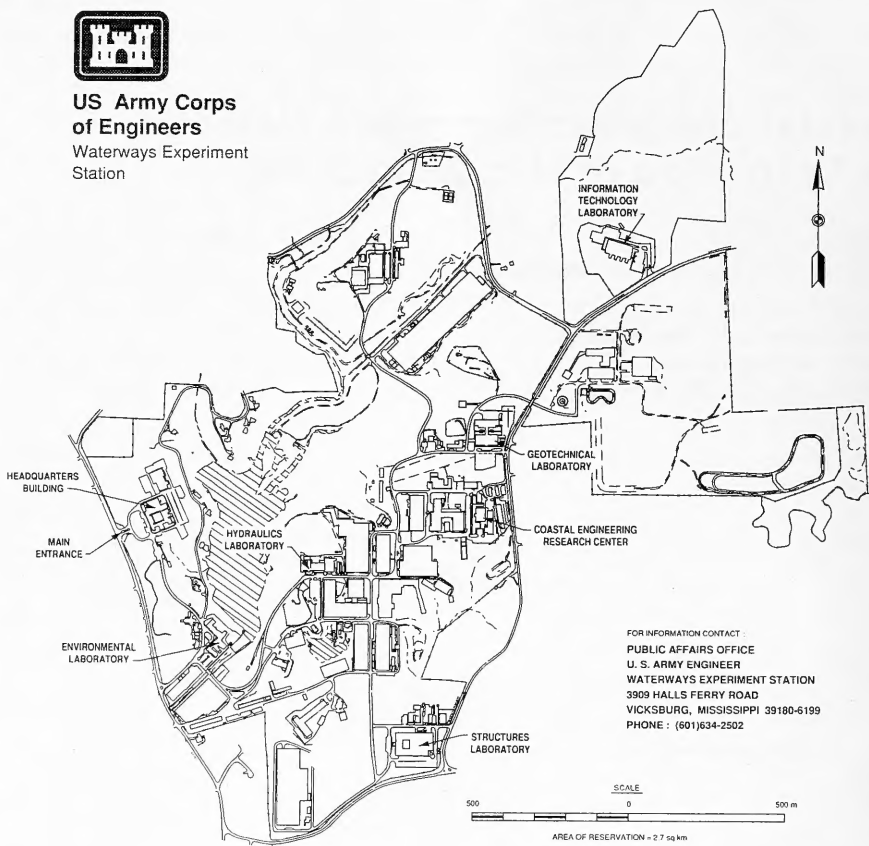
Final report

Approved for public release; distribution is unlimited





**US Army Corps
of Engineers**
Waterways Experiment
Station



FOR INFORMATION CONTACT :
PUBLIC AFFAIRS OFFICE
U. S. ARMY ENGINEER
WATERWAYS EXPERIMENT STATION
3909 HALLS FERRY ROAD
VICKSBURG, MISSISSIPPI 39180-6199
PHONE : (601)634-2502

Waterways Experiment Station Cataloging-in-Publication Data

Fowler, Jimmy E.

Coastal scour problems and methods for prediction of maximum scour / by Jimmy E. Fowler, Coastal Engineering Research Center ; prepared for U.S. Army Corps of Engineers.

65 p. : ill. ; 28 cm. -- (Technical report ; CERC-93-8)

Includes bibliographical references.

1. Scour (Hydraulic engineering) 2. Sea-walls. 3. Underwater pipelines. 4. Rubble mound breakwaters. I. United States. Army. Corps of Engineers. II. Coastal Engineering Research Center (U.S.) III. U.S. Army Engineer Waterways Experiment Station. IV. Title. V. Series: Technical report (U.S. Army Engineer Waterways Experiment Station) ; CERC-93-8.

TA7 W34 no.CERC-93-8

PREFACE

This report was prepared by the US Army Engineer Waterways Experiment Station (WES) Coastal Engineering Research Center (CERC) and is the result of work performed under Coastal Research and Development Program Work Unit 31715, "Laboratory Studies on Scour." This research was authorized and funded by Headquarters, US Army Corps of Engineers (HQUSACE), and was conducted by Dr. Jimmy E. Fowler, Research Hydraulic Engineer, under the general supervision of Dr. James R. Houston, Director of CERC; Mr. Charles C. Calhoun, Assistant Director of CERC; Mr. C. E. Chatham, Chief of the Wave Dynamics Division; and Mr. D. G. Markle, Chief of the Wave Processes Branch. The HQUSACE Technical Monitors for this research were Messrs. J. H. Lockhart, J. G. Housley, D. A. Roellig, and B. W. Holliday.

The report was prepared by Dr. Fowler. The author acknowledges the contributions to this report of the following: Dr. Steven A. Hughes, Research Hydraulic Engineer, CERC; Mr. L. A. Barnes, Mr. J. E. Evans, Engineering Technicians, CERC; and Ms. J. A. Denson and Mr. R. R. Sweeney, Contract Students, CERC.

Director of WES during preparation and publication of this report was Dr. Robert W. Whalin. Commander of WES was COL Leonard G. Hassell, EN.

CONTENTS

	Page
PREFACE	1
LIST OF TABLES	4
LIST OF FIGURES	4
CONVERSION FACTORS, US CUSTOMARY TO METRIC (SI) UNITS OF MEASUREMENT	5
 PART I: INTRODUCTION	 6
General	6
Purpose	6
Background	6
Organization of Report	7
 PART II: GENERAL DISCUSSION OF SEDIMENT TRANSPORT	 8
Sediment Transport Modes	8
Critical Conditions for Sediment Transport Under Unidirectional Uniform Flows	8
Critical Conditions for Sediment Transport Under Oscillatory Flows	10
Critical Depths for Incipient Sediment Motion	14
Bed-Load Transport in Unidirectional Flows	15
Bed-Load Transport Under Wave Action	17
Suspended-Load Transport in Unidirectional Flows	19
Suspended-Load Transport in Oscillatory Flows	20
 PART III: SCOUR PROBLEMS AT COASTAL STRUCTURES	 22
General	22
Scour Problems at Rubble-Mound Structures	22
Scour Problems at Piles or Other Vertical Supports	24
Scour Problems at Vertical Seawalls	25
Scour Problems at Submerged Pipelines	26
 PART IV: SCOUR PREDICTION METHODS	 27
General	27
Scour Prediction at Rubble-Mound Structures	28
Scour Prediction at Piles or Other Vertical Supports	33
Scour Prediction at Vertical Seawalls	35
Rule-of-Thumb Methods	36
Semi-Empirical Methods	36
Other Laboratory Studies to Investigate Scour at Seawalls	43
Field Studies	44
Scour Prediction at Submerged Pipelines	45

PART V: MODELING SCOUR AT COASTAL STRUCTURES USING MOVABLE-BED PHYSICAL MODELS	49
General	49
Model and Prototype Similarities	49
Movable-Bed Modeling Guidance	50
Recent Successes with Movable-Bed Model Studies	51
 PART VI: SUMMARY	 52
Rubble-Mound Structures	52
Vertical Piles and Similar Structures	54
Vertical Wall Structures	54
Submerged Pipelines	55
 REFERENCES	 56
 APPENDIX A: NOTATION	 A1
SF298	

LIST OF TABLES

<u>No.</u>		<u>Page</u>
1	Comparison of Values of α_{crit} and η for Use in Equation 12	14
2	Scour Prediction Methods for Various Scour Modes	53

LIST OF FIGURES

<u>No.</u>		<u>Page</u>
1	Forces on a particle in unidirectional flows	8
2	Curve representing conditions of incipient motion in unidirectional uniform flows	11
3	Komar and Miller (1974) plots of near-bottom orbital velocity for threshold of sediment movement under oscillatory waves (extracted from Hales (1980))	13
4	Einstein's relationship between Φ^* and ψ^* (Herbich et al. 1984)	17
5	Empirical relation for bed-load transport using data of Kalkanis and Abou-Seida (after Hales (1980))	19
6	Scour problems with rubble-mound structures	23
7	Scour problems at vertical piles	24
8	Scour problems at vertical seawalls.	26
9	Scour problems at pipelines	26
10	Composite cross section proposed by Sawaragi (1966)	30
11	Stability number cubed versus relative berm depth from Markle (1989)	31
12	Stability number cubed versus relative berm depth for toe berms fronting rubble-mound structures and rubble toes and foundations for impermeable vertical structures (after Markle (1989))	32
13	Maximum scour depth versus deepwater wave height for vertical seawalls	37
14	Definition sketch for Jones' method	38
15	Predicted scour depths versus measured scour depths using proposed equation with irregular wave data only	41
16	Pipeline scour problem as described by Hennessy and Chao	45
17	Friction factor versus grain Reynolds number	46
18	Maximum pipeline scour as a function of bottom velocity for $d_g = 0.0082$ ft	48

CONVERSION FACTORS, US CUSTOMARY TO METRIC (SI)
UNITS OF MEASUREMENT

US customary units of measurement used in this report can be converted to metric units as follows:

<u>Multiply</u>	<u>By</u>	<u>To Obtain</u>
degrees* (angle)	0.01745329	radians
feet	0.3048	metres
feet per second	0.3048	metres per second
pounds (force)	4.4482205	Newtons
pounds (mass)	0.4535929	kilograms
pounds (mass) per cubic foot	16.01846	kilograms per cubic metre
square feet per second	0.0929	square metres per second

* To obtain Celsius (C) temperature readings from Fahrenheit (F) readings, use the following formula: $C = (5/9) (F - 32)$. To obtain Kelvin (K) readings, use: $K = (5/9) (F - 32) + 273.15$.

COASTAL SCOUR PROBLEMS AND METHODS
FOR PREDICTION OF MAXIMUM SCOUR

PART I: INTRODUCTION

General

1. Scour at coastal structures is a serious problem that causes damage to structures. Coastal engineers have long recognized the consequences of scour at and in the vicinity of the toe of structures, and elaborate and expensive toe protection schemes have often been implemented. In instances where appreciable scour has already occurred, a common solution has been to fill the scour hole with stone or other suitable material. Under certain wave and/or current conditions, the base which supports coastal structures is eroded and partial or total failure can occur. Because it is usually very costly to repair these structures, proper initial design and construction methods that consider scour potential are desirable. This report is concerned with examining existing scour prediction methods for typical coastal structures/facilities.

Purpose

2. The purpose of this report is to review existing methods for scour prediction and to determine which of these methods are most appropriate for the various applications that are of interest to field engineers.

Background

3. Scour in the vicinity of coastal structures has been the subject of research efforts for many years. To adequately study this problem, researchers must address the various effects of waves, wind, tide, currents, and storm surge on both the structure itself and the bed on which the structure resides. Among the most common are problems related to toe scour at rubble-mound structures, scour at the base of piles, toe scour at vertical seawalls, and scour at horizontal pipelines. Prediction methods for these types of scour problems vary from using rules of thumb, to empirically derived equations to theoretically derived relationships. When existing computational methods are insufficient, physical model studies often are performed. For

more complete information on scour studies, consult Kraus (1988), Athow and Pankow (1986), Einstein and Wiegel (1970), and Herbich et al. (1984).

Organization of Report

4. A summary and general discussion of sediment transport are presented in Part II. A description of the most commonly encountered coastal scour problems is presented in Part III. Part IV is a discussion of prediction methods and where appropriate, brief summaries of scour-related studies also are presented. Part V presents a discussion of physical modeling approaches to studying scour (movable-bed) problems. Part VI is a summary of Parts II through V. Appendix A is a listing of the nomenclature used in the report.

Sediment Transport Modes

5. In general, researchers agree that in order to accurately describe sediment transport, it is necessary to consider the forces that initiate sediment motion, subsequent transport, and the path back to the bottom. Typically, sediment moves along the bed in a tumbling fashion as *bedload*, by being lifted higher up into the water column and being moved by the water particles as *suspended load*, or in some combination of the two. The proportion of each mode of transport relative to the total amount of sediment transport depends largely on the density and size of the sediment and the hydraulic domain that acts on the bed. In typical coastal scenarios, where the bed is predominantly non-cohesive sands, suspended transport is prevalent in highly energetic hydraulic regimes, such as in the surf zone.

Critical Conditions for Sediment Transport
Under Unidirectional Uniform Flows

6. In most cases involving sediment transport, it is useful to discuss the concept of critical values associated with the moment at which sediment grain motion is incipient. Most commonly, near-bottom fluid velocities and shear stresses between the fluid and sediment are used to describe what is called the critical point, or the moment just before a sediment particle begins to move. This is examined by an analysis of the forces that act on a particle initially at rest in a unidirectional flow field. Among the significant forces acting on a single particle in a flow situation are the particle's weight and the forces attributed to fluid and particle interaction (drag and lift). Figure 1 schematically depicts these forces as they would occur for a particle positioned on top of other particles. When these forces are in balance or the restraining forces are greater than the net of the forces trying to move the particle, no motion can occur. Analysis of forces acting on a particle in unidirectional flows is fairly straightforward and has been presented adequately in numerous other research efforts (Shields 1936, Silvester 1974, Middleton and Southard 1978, Clark 1979, and Hales 1980). This analysis involves taking moments about a "pivot point" shown as P in the figure and results in the following equation:

$$D (\cos\phi) \frac{d}{2} = (W - L) \sin(\phi) \frac{d}{2} \quad (1)$$

where

- D = drag force, lb_f
d = representative grain diameter, ft

- W = weight of particle, lb_f and
 L = lift force, lb_f

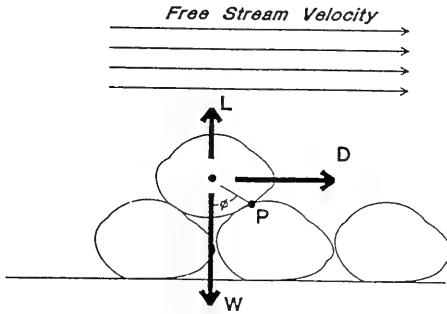


Figure 1. Forces on a particle in unidirectional flows

The value for ϕ is typically assumed to be equal to the angle of repose of the grains. For sand, this value is typically taken between 30 and 35 deg^{**}. The lift force L is typically not considered in the analysis because it is inherently included in turbulent fluctuations. The forces W and D can be written as

$$W = C_1 d^3 (\gamma_{\text{sediment}} - \gamma_{\text{fluid}}) \quad (2)$$

and

$$D = C_2 d^2 \tau_0 \quad (3)$$

where

γ = specific weight, lb_f/ft³

C_1 = "shape" coefficient

C_2 = drag coefficient

τ_0 = boundary shear stress, lb_f/ft²

Combination of Equations 2 and 3 yields an expression for the shear stress given by

$$\tau_0 = \frac{C_1}{C_2} \tan \phi d (\gamma_{\text{sediment}} - \gamma_{\text{fluid}}) \quad (4)$$

Rearranging Equation 4 to obtain τ_0 in dimensionless form results in

** A table of factors for converting non-SI units of measurement to SI (metric) units is presented on page 5.

$$\frac{\tau_0}{d (\gamma_{\text{sediment}} - \gamma_{\text{fluid}})} = \frac{C_1}{C_2} \tan \phi \quad (5)$$

The left-hand side of this equation is commonly referred to as the Shields parameter, after A. Shields, widely acknowledged as the first to develop guidance on criteria for initiation of sediment motion. Experimental studies have shown that the right-hand side (specifically C_1 and C_2) of this equation varies with the boundary or grain Reynolds number R_g . The grain Reynolds number relates the degree to which sediment grains project into the zone immediately above the viscous sublayer of the boundary layer and is typically expressed as

$$R_g = \frac{u_* d}{\nu} \quad (6)$$

where

u_* = apparent or shear velocity, ft/sec

ν = kinematic viscosity, ft²/sec

Plotting experimentally obtained values of the Shields parameter versus the grain Reynolds number yields the well-known Shields diagram. Although the original work of Shields (1936) was done for inorganic particles of uniform size in a unidirectional flow, numerous others have conducted similar research to broaden the applicability of the Shields diagram, with median diameter d_g used to define sediment size. Figure 2 shows a curve fitted to the Shields data as well as data from other investigators. The curve itself represents a reasonable approximation of conditions for impending sediment particle motion in a unidirectional flow. Conditions that plot above the curve correspond to regimes where sediment motion does occur while no motion occurs for conditions which fall below the curve.

Critical Conditions for Sediment Transport Under Oscillatory Flows

7. When the motion of particles in unidirectional flow is compared to the motion of particles subjected to oscillatory flows, obvious differences are seen in both the flow of the fluid and the path of the particle. In steady flows, sediment transport is related to flow characteristics and sediment/fluid properties. In oscillatory flows, additional forces are

exerted on the grains by accelerations and decelerations of the fluid particles in this flow situation. These forces are random in nature and this randomness also is exhibited in associated sediment transport rates and directions. In light of this, dimensional analysis techniques or other means typically are used to obtain relationships and parameters that have empirical coefficients to predict the point of incipient sediment motion. Surprisingly, Madsen and Grant (1975) found that the Shields function for unidirectional flows is also relatively reliable as a general criterion for threshold of movement under irregular flows such as overpassing water waves. As a first-order approximation, linear wave theory may be used to describe near-bottom velocities. However, linear theory assumes purely oscillatory motion, which implies no net sediment transport even if incipient (threshold) velocity requirements are exceeded. It is well known that nonlinear effects are introduced by wave asymmetries, bottom irregularities, and wave-induced mass

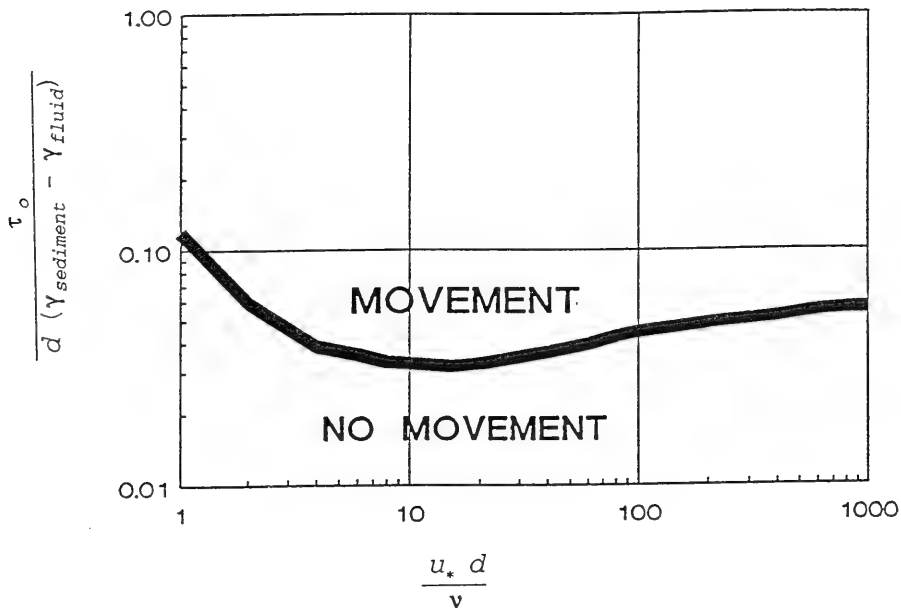


Figure 2. Curve representing conditions of incipient motion in unidirectional uniform flows

transport currents. These effects disturb the equilibrium that would be exhibited by the purely to-and-fro motion assumed by linear wave theory, and result in a net transport of sediment. Additional discussion of this subject may be found in numerous sources (Silvester 1974, Komar and Miller 1974, Madsen and Grant 1975, Middleton and Southard 1978, Hales 1980, and Herbich et al. 1984). For sediments subjected to wave and current action, the time histories of lift and drag forces are much more complex and analysis is far more difficult. In spite of the difficulties, numerous relationships have been developed for critical velocities V_c in oscillatory flows:

$$\begin{array}{l} \text{Hallermeier} \\ (1981) \end{array} \quad V_c = [8 \left(\frac{\gamma_s}{\gamma} - 1 \right) g d_g]^{0.5} \quad (7)$$

$$\begin{array}{l} \text{Eagleson} \\ \text{and Dean} \end{array} (1966) \quad V_c^2 = \frac{4/3 g d_g \left(\frac{\gamma_s}{\gamma} - 1 \right)}{C_D} \tan(\phi_s) \quad (8)$$

$$\begin{array}{l} \text{Madsen and Grant} \\ (1975) \end{array} \quad V_c^2 = \frac{2 \left(\frac{\gamma_s}{\gamma} - 1 \right) g V_s}{C_D A_s} \tan(\phi_s) \quad (9)$$

$$\frac{V_c}{\omega} = \frac{2.5}{\log u_* (d_g/\nu) - 0.06} + 0.66 \quad \text{for } 0 < \frac{u_* d_g}{\nu} < 70$$

$$\begin{array}{l} \text{Yang} \\ (1973) \end{array} \quad (10)$$

$$\frac{V_c}{\omega} = 2.05 \quad \text{for } 70 < \frac{u_* d_g}{\nu}$$

and the relationships of Komar and Miller (1974)

$$\frac{\rho u_{\max}^2}{(\rho_s - \rho) g d_g} = 0.21 (A_o/d_g)^{1/2} \quad \text{for } d_g < 0.05 \text{ cm}$$

$$\begin{array}{l} \text{Komar and} \\ \text{Miller} \end{array} (1974) \quad (11)$$

$$\frac{\rho u_{\max}^2}{(\rho_s - \rho) g d_g} = 0.46 \pi (A_o/d_g)^{1/4} \quad \text{for } d_g > 0.05 \text{ cm}$$

For the above,

- d_g = median grain diameter, ft
- C_D = drag coefficient

- ϕ_s = angle of repose for a given sediment grain, degrees
- γ = specific weight of fluid, lb_f/ft^3
- γ_s = specific weight of sediment, lb_f/ft^3
- V_s = volume of a sediment grain, ft^3
- A_s = projected area of a sediment grain, ft^2
- A_o = orbital diameter of wave motion, ft
- ω = terminal fall velocity of sediment, ft/sec
- u_* = shear velocity = $(\tau/\rho)^{1/2}$, ft/sec
- u_{\max} = near bottom maximum horizontal orbital velocity, ft/sec
- ρ_s = sediment density, lb_m/ft^3
- ρ = fluid density, lb_m/ft^3
- g = acceleration due to gravity, ft/sec^2

The relationships of Komar and Miller are shown graphically in Figure 3 below. Their findings, based solely on laboratory data, essentially state that the threshold of sediment movement for median grain diameter d_g and density ρ_s can be specified by a wave period and a near-bed orbital velocity (u_{\max}). Use of the Komar and Miller relationships should be tempered by the lack of prototype data used to verify them.

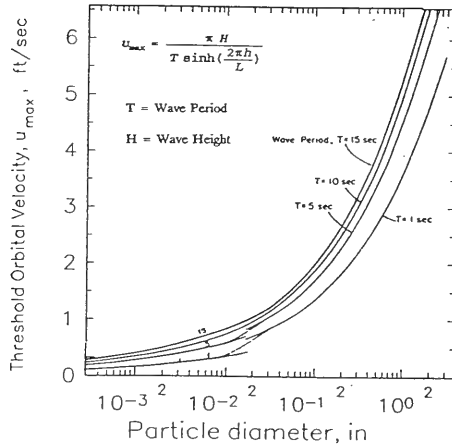


Figure 3. Komar and Miller (1974) plots of near-bottom orbital velocity for threshold of sediment movement under oscillatory waves (extracted from Hales (1980))

Critical Depths for Incipient Sediment Motion

8. In addition to critical velocity, it is often desirable to calculate depths at which sediment transport occurs for oscillatory flows. Several empirical formulas that have been used successfully to calculate critical water depths for sand motion can be summarized in the following form:

$$\frac{H_o}{L_o} = \alpha_{crit} \left(\frac{d_g}{L_o} \right)^\eta \left(\sinh \frac{2\pi h_c}{L_o} \right) \frac{H_o}{H_c} \quad (12)$$

In the above,

H_o = deepwater wave height, ft

L_o = deepwater wave length, ft

α_{crit} = empirically obtained coefficient for critical water depth calculation

d_g = median grain diameter of sediment, ft

η = empirically obtained exponent for critical water depth calculations

h_c = critical water depth, ft

H_c = critical wave height, ft

Table 1 (after Herbich et al. 1984) provides values of α_{crit} and η as empirically obtained by several researchers.

Table 1 Comparison of Values of α_{crit} and η for Use in Equation 12					
Parameter	Sato and Kishi (1954)	Kurihara et al. (1956)	Ishihara & Sawaragi (1962)	Sato, et al. (1963)	
η	1/2	1/2	1/4	1/3	1/3
α_{crit}	10.2	1.56-2.44	0.171	0.565	1.35
Type of movement	General movement	Incipient movement	Incipient movement	Surface layer movement	Completely active movement

Differences among the above values most likely are attributed to the various criteria used by each researcher to establish critical conditions for sediment transport. For example, Sato and Kishi used well-established general bottom motion as their criterion, while Kurihara et al. and Ishihara and Sawaragi

used the point at which sediment particles were first observed to move as their criterion. Sato and Tanaka identified two different criteria to describe critical conditions - the first characterized by surface layer (1-3 grain diameters in depth) movement only and the second by completely active movement in both the surface and supporting layers.

Bed-Load Transport in Unidirectional Flows

9. Although numerous bed-load equations have been suggested, most are concerned with the total shear (bed and fluid) that resists sediment transport. In addition, most agree that bed-load transport q_b can generally be expressed as a function of

$$q_b = f[\tau_o, \tau_c, g, d, \rho_s, \rho, \mu] \quad (13)$$

where

- τ_o = bed or boundary shear stress, lb_f/ft^2
- τ_c = critical boundary shear stress to initiate movement, lb_f/ft^2
- μ = fluid dynamic viscosity, $lb_f \text{ sec}/ft^2$

10. Generally, there have been three basic approaches to studying the bed-load transport problem in unidirectional flows - the duBoys method, the Schoklitsch method, and the Einstein method. These approaches are similar in that each was developed largely from laboratory flume studies, and all empirical coefficients are based on these laboratory studies. These methods are well-documented in other sources, but are briefly summarized here.

11. duBoys analysis The duBoys analysis (duBoys 1879) assumes that layers of the bed move over one another in such a way that the velocity of the elements of each layer decreases linearly with depth. The velocity decreases until it is zero at the top of the layer that does not move, since its frictional resistance is just in balance with the shear force due to motion of the water. The formula developed by duBoys is given below for unit width of bed-load volume q_b with units determined by the coefficient ψ :

$$q_b = \psi \tau_o (\tau_o - \tau_c) \quad (14)$$

In this equation, ψ is a constant which must be determined for a given bed. Although this model has received much criticism, it has frequently been used as a conceptual model. Based on two-dimensional laboratory tests, Straub (1942) used the duBoys analysis method to develop the following expression for

sediment transport per unit width of channel:

$$q_b = (111,000/d_g^{3/4}) S^{1/2} (n/1.5)^3 U^3 \quad (15)$$

For the above,

- q_b = bed-load sediment transport per unit width of channel, $\text{ft}^3/\text{s}/\text{ft}$
- S = channel slope
- n = Manning's roughness coefficient
- U = average water velocity, ft/sec

Rouse (1938) also used the duBoys method to obtain another expression for bed-load transport, using only easily available quantities:

$$q_b = \frac{10 \gamma_s \gamma^2 g^{1/2} (h_u S)^{5/2}}{(\gamma_s - \gamma)^2 d_g} \quad (16)$$

where h_u is the depth of uniform flow. This equation also has the shortcoming that it is based primarily on laboratory flume tests with no field validation.

12. Schoklitsch analysis. The Schoklitsch method for determining bed-load transport uses a hydraulic discharge relation to evaluate the amount of sediment that may be moving within a given channel section. Laboratory observations to determine the discharge conditions for incipient sediment motion were related to actual prototype bed-load measurements and the following relationship for q_{cr} , critical discharge (volume of fluid flow required for initiation of sediment transport) was obtained:

$$q_{cr} = 2.717 (\gamma_s/\gamma - 1)^{5/3} d_g^{3/2} S^{7/6} \quad (17)$$

This value for critical discharge then is related to the bed-load discharge, q_b , in ft^3/sec per ft , and hydraulic discharge q , in ft^3/sec per ft , by

$$q_b = 2500 S^{3/2} (q - q_{cr}) \quad (18)$$

when d_g is in feet. Equation 17, and other slight variations of it, has been used extensively in Europe.

13. Einstein analysis. Einstein's (1950) analysis utilizes statistical methods to account for the instantaneous fluctuations in velocity that occur during turbulent flow. Einstein's work resulted in a formula that incorporated statistical reasoning to relate the rate of bed-load transport to properties of the grain and flow. His relationships were based on the premise that the probability that any single particle, moving at a given time, is related to its fall velocity, size, specific weight, and hydraulics of the flow. This was carried one step further to assess probability of scour or erosion. Einstein felt that the likelihood of erosion is related to the amount of time that instantaneous lift exceeds the weight of the particles being acted upon in the channel section. Einstein's equations for bed-load

transport are given below:

$$\Phi = \frac{q_b}{\rho_s g} \left(\frac{\rho}{\rho_s - \rho} \right)^{1/2} \left(\frac{1}{g d_u^3} \right)^{1/2} \tag{19}$$

where Φ is a dimensionless measure of bed-load transport and d_u represents uniform grain size. Also,

$$\psi = \left(\frac{\rho_s - \rho}{\rho} \right) \frac{d_u}{R_h S} \tag{20}$$

and

$$\Phi = f(\psi) \tag{21}$$

with R_h , the hydraulic radius, defined as the cross-sectional area divided by the wetted perimeter. Since the equations above were developed for uniform grain size, most field uses require adjustment of Φ and ψ . Adjusted values for individual size classes are given as Φ^* and ψ^* in Figure 4, using d_g in Equation 20 to obtain ψ^* .

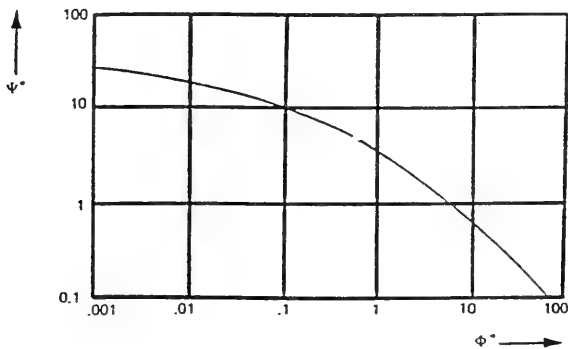


Figure 4. Einstein's relationship between Φ^* and ψ^* (Herbich et al. 1984)

Bed-Load Transport Under Wave Action

14. Einstein's analysis for unidirectional bed-load transport has been used as a building block for analysis of wave-induced bed-load sediment transport. Kalkanis (1963) used the Einstein approach and laboratory tests with an initially plane sand bed to develop approximations for bed-load transport in oscillatory flow regimes. These relationships were further

refined by Abou-Seida (1965) and then by Madsen and Grant (1976) to develop an empirical relationship for prediction of bed-load transport:

$$Y_M = 12.5 (X_M)^3 \quad (22)$$

where Y_M and X_M are dimensionless variables defined by

$$Y_M = \frac{q_b}{\omega d_g} \quad (23)$$

and

$$X_M = \frac{1/2 f_w \rho u_{\max}^2}{\rho g (sg-1) d_g} \quad (24)$$

For the above,

- q_b = bed-load transport rate per unit width, ft³/sec/ft
- ρ = fluid density, lb_m/ft³
- d_g = grain diameter, usually expressed at mean or median, ft
- u_{crit} = orbital near bottom critical horizontal velocity, ft/sec
- ω = sediment fall velocity, ft/sec
- sg = specific gravity of sediment
- f_w = friction factor for wave motion

Swart (1974) expressed the friction factor for wave motion under turbulent conditions as

$$f_w = \exp \left[5.213 \left(\frac{d_e}{a} \right)^{0.194} - 5.977 \right] \quad (25)$$

where a is the wave amplitude and d_e is the equivalent effective bottom roughness, given by

$$d_e = d_g \quad \text{for flat, well-smoothed beds} \quad (26)$$

$$d_e = 2.5 d_g \quad \text{for disturbed, unsmoothed beds} \quad (27)$$

$$d_e = 25 (n_r)^2 / l_r \quad \text{for rippled beds} \quad (28)$$

where

- d_g = median grain diameter, ft
- n_r = ripple height, ft
- l_r = ripple length, ft

Equation 25 is applicable for conditions in which the ratio of wave amplitude to bed roughness exceeds 1.7. The data and curve fit to the data are shown in Figure 5.

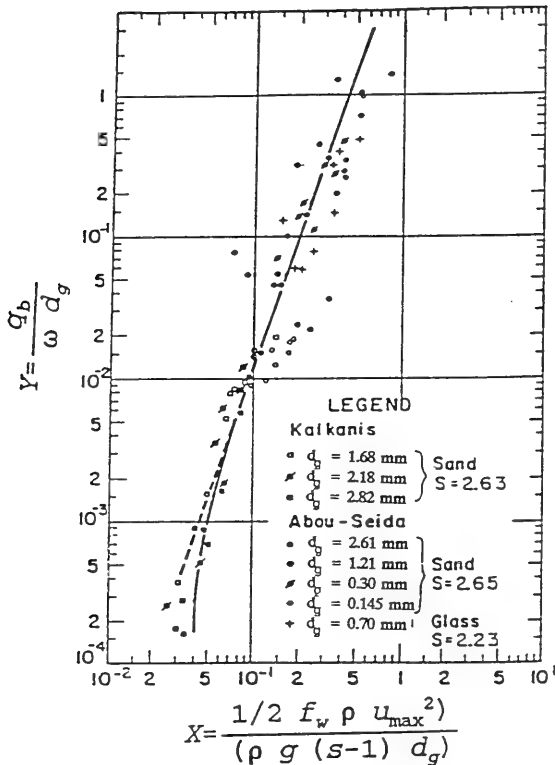


Figure 5. Empirical relation for bed load transport using data of Kalkanis and Abou-Seida (after Hales (1980))

Suspended-Load Transport in Unidirectional Flows

15. Numerous cases exist where suspended load in unidirectional flows is as important as bedload to the overall sediment transport rate. To describe sediment transport dominated by suspended load, one must consider the same parameters used to describe bed-load transport, as well as an additional property of the particle and fluid, known as sediment fall speed. The

additional parameter to be added is ω , the particle fall velocity, in feet per second. For suspended sediment transport, particles in suspension fall by gravity to the bed, where they subsequently are returned to the flow by turbulence and transported by currents. During "equilibrium" or non-eroding conditions, the amount of sediment falling into an area is equal to the amount being carried out of the area. A conservation of mass equation can be written for a given horizontal area of bed such that

$$\omega C_s + \epsilon \frac{dC_s}{dz} = 0 \quad (29)$$

where

C_s = sediment concentration in the water, lb_m/ft³

ϵ = diffusion coefficient

z = distance above bed, ft

Equation 29 is the basic differential equation for suspended sediment transport and can be solved for certain cases if appropriate assumptions are used.

16. Lane and Kalinske (1941) used the assumptions that the diffusion coefficient is constant through the vertical section and equal to the average value determined in terms of the von Karman constant and previously defined shear velocity u_* . Their solution for Equation 29 is given below:

$$C_s/C_A = [(h/z - 1)/(h/A - 1)]^{\omega/0.4u_*} \quad (30)$$

where C_A is a known concentration (in units consistent with C_s) at height A, in ft above the bed, and h is depth of flow, in feet. This equation has been shown to produce relatively accurate results, but is applicable only for equilibrium conditions for a known sediment size.

Suspended-Load Transport in Oscillatory Flows

17. Unlike unidirectional flows, analysis of suspended transport by oscillatory flows is quite complex. Periodic turbulence-induced variations in the direction and velocity of the water particles result in a non-homogeneous region of water/sediment above the bottom. Due to the complexity of this problem, research efforts primarily have resulted in empirical relationships that attempt to relate wave characteristics (height and period), water depth, sediment characteristics, and bottom roughness. Based on laboratory flume studies, MacDonald (1973) found that concentration distribution C_s (lb/ft³) in an oscillating flow could be estimated by

$$\frac{C_s}{C_o} = \exp(M Y) \quad (31)$$

where Y is the elevation above the bottom (feet) and C_o in lb_m/ft^3 (as previously determined by Kalkanis (1963)), and M in ft^{-1} are given by

$$C_o = \frac{(0.618 q_b)}{2 d u_{\max}} \quad (32)$$

$$M = 11.53 U^{-18.45} \quad (33)$$

For the equations above, q_b is computed from previously presented methods and:

- U = average flow velocity, ft/sec
- u_{\max} = maximum near-bottom horizontal particle velocity, ft/sec
- d_g = mean grain diameter, ft

18. Other researchers have used field data to develop equations that relate suspended sediment concentrations to relative wave height. Based on field data obtained near Price Inlet, South Carolina, by Kana (1978), suspended sediment concentrations can be adequately described by

$$\text{Log}_{10}(SS_{10}) = 2.02 - 2.0 \left(\frac{h_b}{H_b} \right) \quad (34)$$

where

- SS_{10} = suspended sediment concentration at 10 cm above the bed, lb_m/ft^3
- h_b = depth of water at point of wave breaking, ft
- H_b = breaking wave height, ft

Other controlling factors included distance relative to the wave breakpoint, beach slope, and deepwater wave height. It was found that mean suspended sediment in the breaker zone correlated well with beach slope and reached a maximum a few yards landward of the breaker line, and for the range of beach slopes studied (0.004 to 0.04) the following relationship was developed

$$\text{Log}_{10}(SS_{10}) = 1.425 + 14.5 m \quad (35)$$

where m is the beach slope given by the decimal fraction of rise over run.

PART III: SCOUR PROBLEMS AT COASTAL STRUCTURES

General

19. One of the major problems associated with design of effective coastal erosion control on navigational assistance structures is being able to, adequately address forces associated with wave attack and associated currents. This continual attack often results in degradation of the base that supports the structure. Numerous cases have been documented where structures have deteriorated and failed due to such a degradation of the foundations by excessive localized erosion of the base, or scour. Generally, scour is defined as the deformation of a flow boundary through removal of materials by a hydraulic flow. For scour to occur in coastal environments, three basic elements must exist. First, there must be an erodible bottom. Second, there must be sufficient energy present to cause the erodible bottom to move and be carried away. Finally, there must be a structure or structural foundation that is built on the erodible bottom. Problems occur when a structure is placed on the seafloor, because existing "equilibrium" conditions are perturbed, and responses such as increased velocities and turbulence may result. Increased velocities and associated turbulence represent increased ability to initiate and sustain sediment particle motion. It is clear that many different conditions can result from a combination of these factors, with each likely to present a unique scour potential. It is clear that unless structures built in scour-prone areas are protected or designed to withstand maximum scour depths, the structure is likely to be undermined and doomed to some degree of failure. Because it would be impractical, if not impossible, to discuss all cases, this summary will be limited to the most commonly occurring coastal scour problems.

Scour Problems at Rubble-Mound Structures

20. For additional discussions of problems common to rubble-mound structures, consult Markle (1986 and 1989), Eckert (1983), and the Shore Protection Manual (SPM) (1984). In a survey of problems with rubble-mound structures conducted in 1984-1986, Markle concluded that the majority of failures begin with damage to the toe of these structures (Figure 6). In general, there are three major problems that occur at most rubble-mound structures experiencing some degree of degradation:

- a. Improper placement and sizing of the toe buttressing stone.

- b. Improper design of toe berms.
- c. Erosion of the bottom material.

Toe-buttrussing stone is used to stabilize the slope armor by preventing downslope slippage of the armor layer and typically is not concerned with scour-related problems, as are items b. and c. The most recent guidance available for design of structures which addresses the three problems listed above is contained in Markle (1989). Generally, sufficient guidance is given for design of bedding or filter layers based on soil type, but very few data are available for selecting material size and geometric configuration for proper toe berm and buttressing design. Although any of the three preceding problems can occur no matter how well the toe of the structure is designed, failure can be expected to occur if the bottom material is exposed to sufficient energy for scour to take place. Additional guidance for design of rubble-mound structures is contained in Pilarczyk (1989) and the SPM (1984). In many cases, the present solution (in some cases impractical) is to extend the berm to some point where insufficient energy exists to displace the bottom materials.

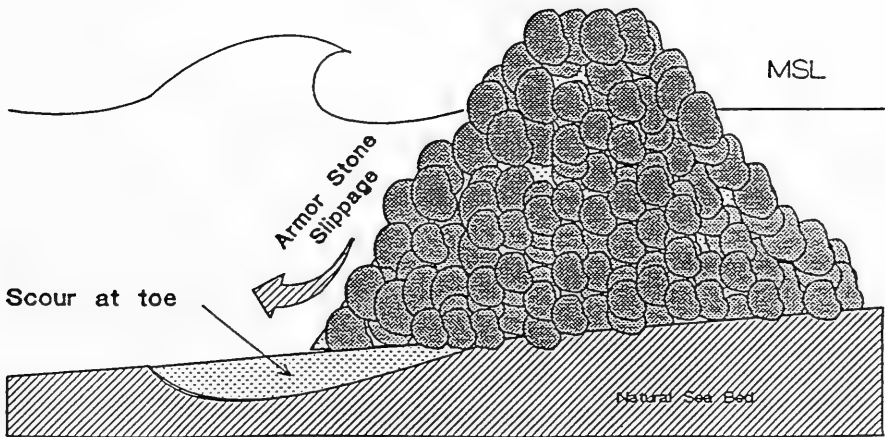


Figure 6. Scour problems at rubble-mound structures

Scour Problems at Piles or Other Vertical Supports

21. For additional discussion of scour problems at and near piles, consult Herbich et al. (1984) and Einstein and Weigel (1970). The problem exists at piles because the structure causes the flow to accelerate as it moves past the structure itself. In this case, vortices are usually generated as the flow moves away from the obstruction, and it is the combination of these effects which causes the sediment particles to become dislodged and subsequently moved away from the structure. Research has shown, and it is fairly obvious, that the greatest rates of scour occur where the fluid velocity is greatest. Also, because the sediment slides down the upstream slope and is deposited on the downstream slope, the walls of the scour hole are typically at an angle roughly equal to the angle of repose (Figure 7).

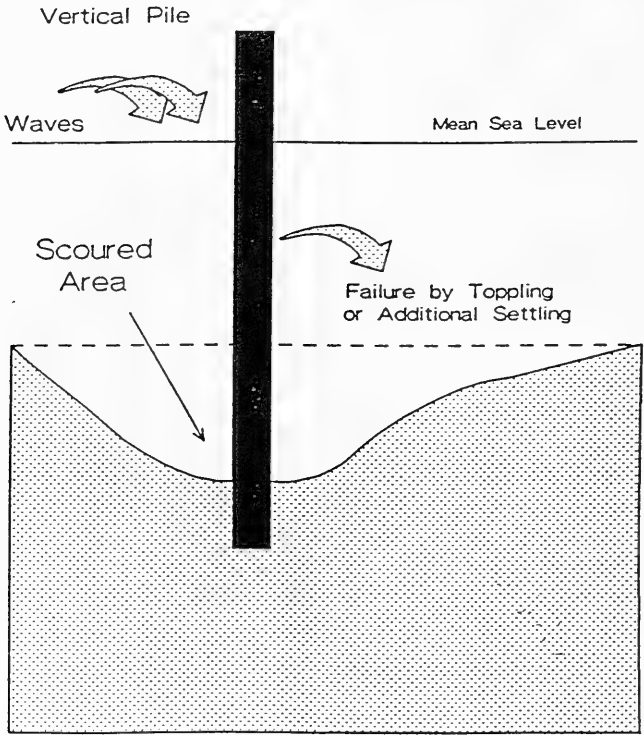


Figure 7. Scour problems at vertical piles

22. In riverine situations, piles are typically driven to bedrock to a layer which is not expected to move, whereas in coastal or offshore situations, construction conditions and distance to bedrock often preclude being able to base the piling on firm foundations. Because of this, scour around piles in this environment is more critical and should be given greater consideration in design of the structure. Scour holes associated with non-oscillatory flow (such as is found in rivers) differ from those found near pier pilings where waves and associated currents supply the energy for sediment transport. In riverine situations, the transport is in the direction of the current. In a wave/current climate, however, the transport, while generally in the direction of the angle of approach of the waves, may also be affected by longshore currents, reflected waves, etc. Laboratory and field studies have been conducted to determine the maximum depths of scour for various situations, and most show that the maximum depth is related to several variables including sediment mean diameter, wave height and period, still-water depth, sediment density, angle of repose of sediment, dimensions of the structure, elapsed time, and the free stream velocity.

Scour Problems at Vertical Seawalls

23. Perhaps the most common of all coastal protection structures is the vertical seawall. Under certain wave and/or current conditions, the base which supports vertical seawalls can be eroded and partial or total failure can occur. To properly design such structures, it is important to be able to estimate the potential depth of scour at the toe. The problems associated with a vertical structure in the presence of a wave climate are amplified by the reflected wave energy that can accompany such a structure. The net result of wave reflection usually is to increase the depth to which the wave can influence the bottom. In most cases where scour at vertical seawalls has caused failure, sand or sediment was eroded beyond or near the bottom of the structure (Figure 8). Following this, the incoming waves exert pressure on the upper part of the structure and failure occurs when the sediment at the toe of the wall is scoured to the point where its resisting ability is overcome by the wave forces and any back pressure exerted on the wall. For additional discussion on the problem of scour at vertical seawalls or other vertical wall structures, consult Fowler (1992), Kraus (1988), Athow and Pankow (1986), Powell (1987), and Herbich et al. (1984).

24. Another case where scour at vertical walls is a problem occurs as a result of tidal or river-related flows. In this case, there may be some wave action on the walls (typically from boat or ship traffic) but the predominant scouring force is the current at the base of the structure. Here, sediment is moved from the base and not replaced. When this occurs over an extended

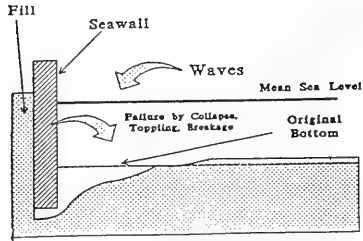


Figure 8. Scour problems at vertical seawalls

period of time, the foundation of the wall is removed and the structure collapses from its own weight. To combat this, stone aprons often are used to harden the toes against scour and help preserve the foundation.

Scour Problems at Submerged Pipelines

25. Another situation where scour presents a problem for coastal engineers and oceanographers is the case of scour under and around submerged pipelines. For additional discussion of this problem, consult Herbich et al. (1984) and Hales (1980). Scour around pipelines occurs in much the same fashion as with pilings in that the flow is accelerated as it moves around and over the structure. This increased velocity, and eddies which accompany it, result in localized areas of scour that expose portions of the pipeline, which in turn leads to other problems, including attachment by barnacles (which increases the surface area exposed to flow as well as increasing drag, exposure to increased flow forces, and loss of protection afforded by the sediment that originally covered it. In the majority of these cases, the problem results from improper installation of the pipe. Most often the pipe is not buried to design depths or is not buried at all. When this is the case, scour holes will usually develop and expose the pipeline to the damage mechanisms previously mentioned (Figure 9).

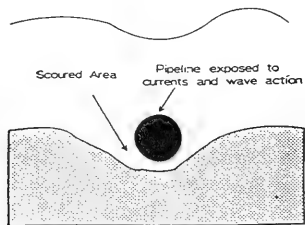


Figure 9. Scour problems at pipelines

General

26. For many scour problems, the primary concern is the amount of scour that will occur, both in terms of area and depth. Depth of scour S_d has been studied by numerous investigators and a functional relationship is:

$$S_d = F_1(\rho, \rho_s, d_g, g, \omega, h, U, v, H, T, \mathcal{L}, L) \quad (36)$$

where

- d_g = median grain diameter, ft
- u = near bottom maximum horizontal orbital velocity, ft/sec
- \mathcal{L} = characteristic size of structure, ft
- H = wave height, ft
- T = wave period, sec

Now, through dimensional analysis techniques, Equation 33 may be reduced to the following dimensionless parameters:

$$\frac{S_d}{h} = F_2 \left[\frac{\rho_s}{\rho}, \frac{d_g}{h}, \frac{U}{\omega}, \left(\frac{\rho_s - \rho}{\rho} \right) \left(\frac{g d_g}{U^2} \right), \frac{UT}{\mathcal{L}}, \frac{U d_g}{v}, \frac{\omega T}{H} \right] \quad (37)$$

A more common expression for dimensionless scour depth in cases where waves are important is given by the ratio of scour depth to wave height, S_d/H . In the above equation, the effect of ρ_s/ρ is accounted for in the fourth parameter in Equation 34 so that the first parameter may be dropped. Additionally, when sediment particle size is small compared to water depth, the second term can be neglected as well. Finally, studies by Carpenter and Keulegan (1958) showed that for oscillatory flows, scour at the bed was not strongly related to the Reynold's number, so that the next-to-last term may also be omitted. As before, dimensionless quantities may be formed as shown below:

$$\frac{S_d}{H} = F_3 \left[\frac{U}{\omega}, \left(\frac{\rho_s - \rho}{\rho} \right) \left(\frac{g d_g}{U^2} \right), \frac{UT}{\mathcal{L}} \right] \quad (38)$$

From the above relationship, near-bottom fluid velocity, sediment fall velocity, relative sediment density ($(\rho_s - \rho)/\rho$), sediment particle mean diameter, wave height, wave period, and characteristic structure length are generally the most important parameters for description of local scour. Under

more specific scour regimes such as scour at vertical seawalls, additional assumptions can be made that result in an additional reduction of important parameters.

Scour Prediction at Rubble-Mound Structures

27. Depth of scour at the toe of rubble-mound structures is extremely difficult to isolate and measure. This is due to the subsidence or lowering of the stone (or other materials from which the structure is constructed) which accompanies scouring of the toe foundation. This subsidence typically fills the void caused by scoured sediment and makes direct measurement of the actual scoured depth virtually impossible. In light of this, very few researchers have attempted to develop prediction equations for depth of scour at toes of rubble-mound structures. According to the SPM (1984), "No definitive method for designing toe protection is known," however, Markle (1989) does provide design guidance for toe berm armor for stability, even though scour-related problems are not addressed. Usually, general or approximate guidelines based on laboratory and field studies are used to design jetties, breakwaters, and revetments that have varying degrees of toe scour protection. Most often, the type and amount of toe scour protection is given as a rule of thumb or in terms of the mean weight of the individual stable armor unit. This mean weight of the stable individual armor unit W_a , lb_r, is determined by various empirically derived equations, the most common of which is that developed by Hudson (1961):

$$W_a = \frac{\gamma_r H_D^3}{K_D (S_r - 1)^3 \cot \theta} \quad (39)$$

For the above, γ_r is the specific weight of armor unit, H_D is the design wave height at the structure site, S_r is the specific gravity of the armor unit relative to the water at the structure given by $S_r = \gamma_r/\gamma$, where γ is the specific weight of the water, θ is the angle (in degrees) of the structure slope measured relative to the horizontal plane, and experimentally determined K_D is the stability coefficient which varies with the type of armor unit as well as other parameters. The reader is advised to consult the Shore Protection Manual for additional information regarding the use of Equation 36.

28. The following section briefly describes various methods for approximating amounts of scour and, where appropriate, recommended guidelines for planning toe protection methods. For additional information on scour at rubble-mound structures, consult Sawaragi (1966), Hales (1980), Eckert (1983),

the Shore Protection Manual (1984), Herbich et al. (1984), and Markle (1986 and 1989).

29. Sawaragi (1966) was among the earliest researchers to attempt to estimate toe scour at rubble-mound structures. In his studies, numerous 2-D tests were conducted using a permeable plate having holes sufficient to simulate appropriate void ratios to isolate scour depth from subsidence and subsequently determine the effect of various parameters on structure subsidence and toe scour. Sawaragi found that a relation existed between the void ratio of the structure, the coefficient of wave reflection, and depth of scour. Generally, results reported indicated that although the reflection coefficient, $K_r = H_r/H_i$, was roughly constant for void ratios greater than 20 percent, it increased quickly for smaller values of void ratio. H_r and H_i are reflected and incident wave heights, respectively. Also, relative scour depth S_d/H_o increased with increasing reflection coefficient, with a break point marked by $K_r = 0.25$, where values of K_r less than 0.25 experienced significantly less scour than structures with K_r greater than 0.25. For breaking waves, Sawaragi noted that depth of scour is not the result of a constant process - it is rather a process interspersed with episodic accretion and erosional events. Finally, Sawaragi found that maximum scour depth occurs in water depths approximately equal to one half the incident deepwater wave height. This conclusion was based solely on one set of wave conditions and may be suspect. Based on the above findings, Sawaragi proposed a composite cross section similar to that shown in Figure 10 where l is calculated by the following:

$$l = \frac{h_2 + R}{\tan 20^\circ} - s(R + h_1) - s'(h_2 - h_1) \quad (40)$$

and

$$l = \frac{h_2 + R_c}{\tan 20^\circ} - s(R_c + h_1) - s'(h_2 - h_1) \quad (41)$$

where R is height from seawater level to the limit of wave runup and R_c is the height of the top of the structure relative to sea level when the structure is overtopped; h_1 , h_2 , s and s' are as shown in Figure 10. Equation 40 is used for cases where the top of the permeable structure is higher than the upper limit of wave runup and Equation 41 is used in cases where the top of the permeable structure is lower than the upper limit of wave runup.

30. Hales (1980) conducted a survey of scour protection practices in the United States and found that a rule of thumb for minimum toe scour protection is a toe apron measuring 2.0 to 3.0 ft thick and 4.8 ft wide. In the northwest United States (including Alaska), aprons are commonly 3.0-5.0 ft thick and 10.0-25.0 ft wide. Materials used vary from quarry-run stone up to 1.0 ft in diameter to gabions 1.0 ft thick.

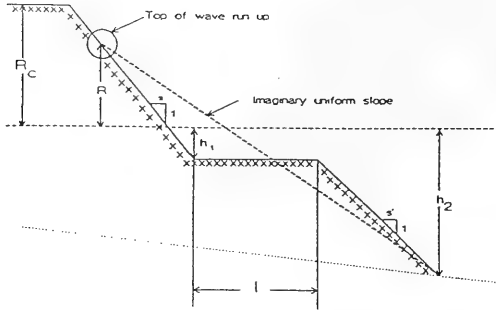


Figure 10. Composite cross-section proposed by Sawaragi (1966)

31. Based on a study by Eckert (1983), toe scour protection should be designed to accommodate the maximum scouring force that exists where wave downrush on the structure face extends to the toe. According to Eckert (1983), the rule of thumb for minimum toe scour protection will be inadequate if the following conditions are present:

- a. The water depth at the toe of the structure is less than twice the height of the maximum unbroken wave height that can exist in that water depth.
- b. The wave reflection coefficient exceeds 0.25, which is generally true for structures having slopes steeper than 1 on 3.

32. Movable bed model tests conducted by Lee (1970, 1972) on a quarrystone-armored jetty with a slope of 1 vertical on 1.25 horizontal indicated that adequate toe protection was provided by a double layer of rock having mean weight W_{apron} , given by

$$W_{apron} = W_a / 30 \quad (42)$$

where W_a is the mean weight of individual primary armor stone, lb_f , as determined from Equation 39. In addition, tests showed that the width of the toe protection should be equal to the width of four to six of the stones having the mean weight given by Equation 42, and could be estimated by the following:

$$B_{apron} = n_s k_{\Delta} \left(\frac{W_{apron}}{\gamma_r} \right)^{1/3} \quad (43)$$

In the above, B_{apron} is the apron width in feet, n_s is the number of stones, and k_{Δ} is a layer coefficient varying between 0.94 and 1.15, dependent upon armor type, shape, and construction method as detailed in the Shore Protection Manual (1984), and γ_r is the unit weight of armor stone, lb_f/ft^3 .

33. Recently, laboratory scaled model studies were conducted by Markle (1989) to address the sizing of toe berm and toe buttressing stone in breaking wave environments. These tests resulted in the most recent guidance for sizing toe berm armor stone and toe buttressing stone. Basically, guidance is given in terms of the stability number N_s , defined by

$$N_s = \left(\frac{\gamma_{rb}}{W_{50}} \right)^{1/3} \frac{H_D}{(S_r - 1)} \quad (44)$$

with W_{50} , the median weight of individual berm stone in lb_f , as defined previously in Equation 39. In addition,

- γ_{rb} = specific weight of berm stone, lb_f/ft^3
- S_r = specific gravity of berm stone relative to the water in which the structure resides, i.e., $S_r = \gamma_{rb}/\gamma$
- H_D = design wave height, ft
- γ = specific weight of water in which structure resides, lb_f/ft^3

Basically, the guidance for toe berm stone states that "unless site-specific model tests are conducted to justify higher values of N_s , stability number should be selected based on the lower limit curve presented in Figures 11 and 12, and the individual toe berm armor stone weights should range from a maximum of $1.3 W_{50}$ to a minimum of $0.7 W_{50}$." For toe buttressing stone, limited 2-D stability tests for toe buttressing a one-layer uniformly placed tri-bar structure, a stability number N_s equal to 1.5 should be used in a wave-breaking environment.

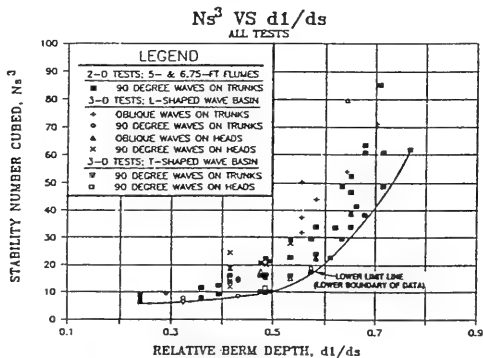
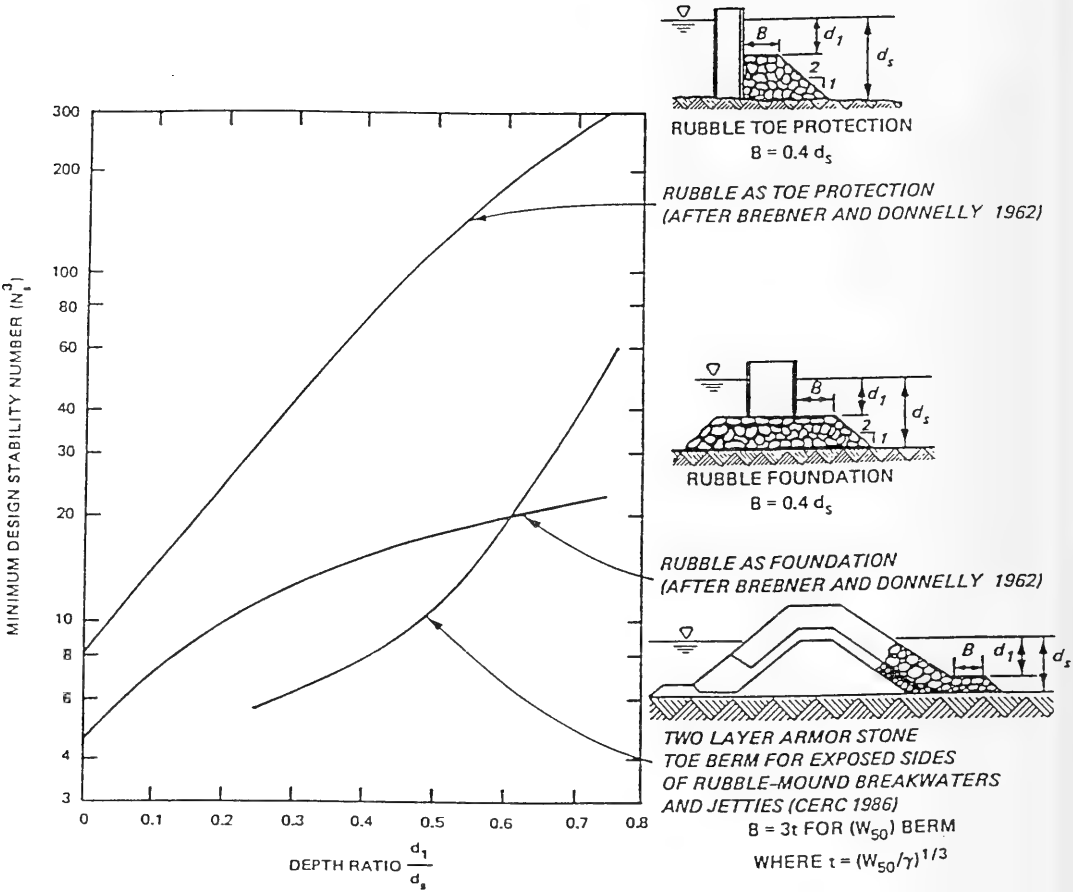


Figure 11. Stability number cubed versus relative berm depth from Markle (1989). (See Figure 12 for definition of d_1 and d_s)



NOTE: N_s^3 VALUES FOR TOE BERMS FRONTING RUBBLE-MOUND STRUCTURES ARE FOR BREAKING WAVE DESIGN CONDITIONS.

Figure 12. Stability number cubed versus relative berm depth for toe berms fronting rubble-mound structures and rubble toes and foundations for impermeable vertical structures (after Markle (1989))

Scour Prediction at Piles or Other Vertical Supports

34. For a more complete description of scour prediction methods for scour at vertical piles, consult Herbich et al. (1984) and Einstein and Weigel (1970). Based on test results from a laboratory study in which 39 flume tests were run to examine effects of waves, currents, and the combination of the two, Herbich et al. concluded that scour at the base of vertical piles caused by wave action alone is insignificant and proposed the following:

For *local scour*, S_1 , in ft, which occurs in the immediate vicinity of the obstruction causing the scour:

$$\log_{10} \left(\frac{S_1}{h} \right) = -1.2935 + 0.1917 \log_{10} \beta \quad (45)$$

where

$$\beta = \frac{H_o^2 L_o u_b^3 D_p [u_b + (1/T - u_b/L_o) H_o L_o / 2h]^2}{[(\rho_s - \rho) / \rho] v g^2 h^4 d_g} \quad (46)$$

In the above,

D_p = pile diameter, ft

u_b = near-bottom current velocity, ft/s

For *total scour depth*, S_t , in ft, which occurs over a much larger area and includes local and general scour:

$$\log_{10} \left(\frac{S_t}{h} \right) = -1.4071 + 0.2667 \log_{10} \beta \quad (47)$$

For the 39 tests conducted, the correlation coefficient r for Equation 45 was reported to be 0.970 and 0.905 for Equation 47. In addition to the above equations, an additional parameter α , which can be used to determine whether general scour will occur, was developed and is given as:

$$\alpha = \frac{H_o^2 L_o u_b^2 [u_b + (1/T - u_b/L_o) H_o L_o / 2h]^2}{[(\rho_s - \rho) / \rho] g^2 h^4 d_g} \quad (48)$$

According to Herbich et al., general scour will not occur when $\alpha < 0.02$ and total scour will be limited to that associated with local scour. The above relations were not verified using prototype data. A useful relationship between α and β is

$$\beta = \frac{u_b D}{\nu} \alpha \quad (49)$$

Example 1. Calculate local and total scour associated with a vertical pile given the following information:

$$\begin{aligned} D_p &= \text{pile diameter} = 2.0 \text{ ft} \\ H_o &= 6.0 \text{ ft} \\ T &= 7.5 \text{ sec} \\ h &= \text{depth} = 20.0 \text{ ft} \\ d_g &= 0.25 \text{ mm} = 0.00082 \text{ ft} \\ \rho_s &= \text{sediment density} = 2.65 \text{ lb/ft}^3 \\ \rho &= \text{fluid density} = 1.00 \text{ lb/ft}^3 \\ \nu &= \text{kinematic viscosity} = 0.00001 \text{ ft}^2/\text{s} \\ u_b &= \text{near bottom current velocity} = 1.50 \text{ ft/s} \end{aligned}$$

Solution: The initial step is to determine whether scour will be confined to the immediate vicinity of the pile or if general scour will also occur. This is accomplished by calculating the parameter α :

First, determine the wavelength from the widely known relation

$$L_o = 5.12T_o^2 = 184.0 \text{ ft}$$

Then from Equation 48,

$$\begin{aligned} \alpha &= \frac{(6.0)^2 184.0 (2.0)^2 [2.0 + (1/6.0 - 2.0/184.0) 6.0 (184.0)/2(20)]^2}{[(2.65 - 1.0)/1.0] (32.2)^2 (20.0)^4 (0.00082)} \\ &= 4.68 \end{aligned}$$

Since α is greater than 0.02, general scour will also occur. Equation 45 will be used to calculate local scour but first Equation 49 is used to calculate β :

$$\begin{aligned} \beta &= \frac{u_b D}{\nu} \alpha \\ &= \frac{(2.0)(2.0)}{0.000015} (4.68) \\ &= 152,000 \end{aligned}$$

Now, from Equation 45

$$\begin{aligned}\log_{10}\left(\frac{S_1}{20}\right) &= -1.2935 + 0.1917 \log_{10}(152,000) \\ &= -0.300\end{aligned}$$

so that

$$\begin{aligned}S_1 &= 20 (10)^{-0.300} \\ &= 10.02 \text{ ft}\end{aligned}$$

By a similar method, total scour depth is determined to be

$$\begin{aligned}\log_{10}\left(\frac{S_2}{20}\right) &= -1.4071 + 0.2667 \log_{10}(152,000) \\ &= -0.025\end{aligned}$$

so that

$$\begin{aligned}S_2 &= 20 (10)^{-0.025} \\ &= 18.87 \text{ ft}\end{aligned}$$

Thus, local scour depth will be approximately 10 ft and the total scour will be approximately 19 ft.

Scour Prediction at Vertical Seawalls

35. Researchers have typically developed non-dimensional relationships for predicting scour, typically expressing relative scour in terms of ratio of scour depth to incident deepwater wave height, S_d/H_0 . The following section briefly describes various prediction methods, laboratory studies, and field studies concerning prediction of scour at vertical structures in a wave environment. The following paragraphs present various methods previously developed to predict scour depths in front of vertical seawalls. In general, these methods can be classified as being either rule-of-thumb or semi-empirical methods. Where appropriate, sample calculations are provided, with similar design parameters used to allow comparison of results among the various methods. For additional discussion on prediction of scour at vertical seawalls, consult Herbich et al. (1984), the SPM (1984), Jones (1975), Walton and Sensabaugh (1979), Barnett (1987), Powell (1987), Kraus (1988), and Fowler (1992).

Rule-of-Thumb Methods

36. Based on limited field observations, the most commonly used rule of thumb states that maximum scour depth below the natural bed is roughly less than or equal to the height of the unbroken deepwater wave height, or $S_{\max}/H_o \leq 1$. Data from 2-D laboratory tests conducted at the US Army Engineer Waterways Experiment Station Coastal Engineering Research Center (CERC) by Fowler (1992) fit within the bounds of this rule of thumb. These tests were conducted using a wave flume with no currents and irregular waves on a sand bed. The Fowler data are shown combined with data from other researchers in Figure 13. As can be seen from the figure, some of the data from others exceeds this rule of thumb. In each case, the laboratory tests by others were conducted using regular waves on a sand bed. To investigate this further, the CERC tests were extended to include monochromatic waves having similar heights and periods. In all cases, scour depths associated with the monochromatic tests exceeded scour depths associated with the irregular wave results by an average of 15 percent.

37. Dean (1986) used the "principle of sediment conservation" to develop an "approximate principle" to predict the volume of local scour that would occur during a 2-D situation (e.g., storm-dominated onshore-offshore sediment transport). Dean proposed that the total volume of sediment lost from the front of a structure would be equal to or less than the volume which would have been lost if the structure were not constructed. In other words, the amount (volume) of scour immediately in front of the structure would be less than or equal to the volume of sediment which would have been provided from behind the wall, had it not been there.

Semi-Empirical Methods

38. Jones (1975) used a number of limiting assumptions (including an infinitely long structure and perfect reflection from the wall) to derive an equation for estimation of scour depth at the toe of vertical walls. Jones' equation relates ultimate scour depth S_d to breaking wave height H_b and X_s , the dimensionless location of seawall relative to the intersection of mean sea level and the beach profile. Jones defined X_s as follows:

$$X_s = \frac{X}{X_b} \quad (50)$$

where X is the distance of the seawall from the point of wave breaking and X_b is the distance of the point of wave breaking from the intersection of MSL with the pre-seawall beach profile (see Figure 14). Both distances are

Scour Depth vs Deep Water Wave Height Pooled Data Set

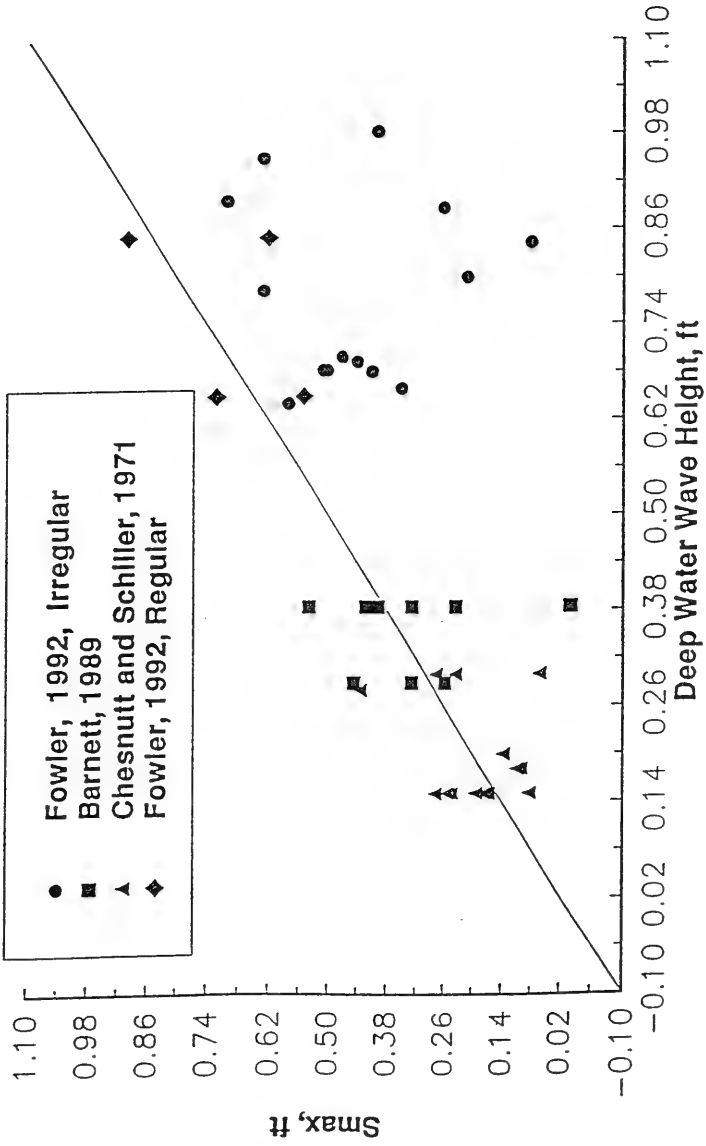


Figure 13. Maximum scour depth versus deepwater wave height for vertical seawalls

derived for the pre-seawall condition and may be determined by the commonly used method presented in the SPM (1984). When the location of the toe of the seawall coincides with the location of mean sea level, $X_s = 1$. The following empirical equation was proposed for prediction of maximum scour depth:

$$\frac{S_{\max}}{H_b} = 1.60 (1 - X_s)^{2/5} \quad (51)$$

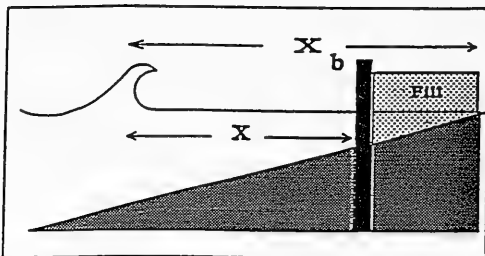


Figure 14. Definition sketch for Jones' method

A major problem with the Jones equation is that zero scour is predicted when the seawall is located at $X_s = 1$ (at the shoreline). This is contradicted in every study examined; in fact, some have found that this seawall location corresponds to the greatest scour condition. This suggests that use of this equation should be limited to conditions where $X_s < 1.0$.

Example 2. For the following given initial design conditions, calculate maximum scour depth.

- $d_g = 0.25$ mm
- $m =$ beach slope in front of seawall = 1:20 = 0.05
- $H_o = 6.0$ ft
- $T_o = 7$ sec
- $h_w =$ depth at base of wall = 2.0 ft

Solution: Initial calculation to be made is determination of X_s as

$$\begin{aligned} X_s &= \frac{X}{X_b} \\ &= \frac{5.0}{10.0} = 0.5 \end{aligned}$$

The first step is to determine H_b and h_b , the depth of water at the point of wave breaking, so that X_b can be determined. The SPM (1984) provides a method for determining H_b and h_b provided H_o , T_o , and the beach slope are known. The method uses Goda's (1970) empirically derived relationships between H_b/H_o and H_o/L_o for a given beach slope. From linear wave theory,

$$\begin{aligned} L_o &= 5.12 T_o^2 \\ &= 250.88 \text{ ft} \end{aligned} \quad (52)$$

so that $H_o/gT_o^2 = 0.0038$. From the SPM (1984)

$$H_b/H_o = 1.28$$

so that $H_b = 7.68 \text{ ft}$ and

$$H_b/gT^2 = 0.00487$$

Also from the SPM

$$H_b/h_b = 1.0$$

so that $h_b = 7.68 \text{ ft}$.

Since the beach slope is 0.05, the distance from the pre-seawall msl/beach profile intersection to the point of wave breaking can be obtained by dividing the depth of breaking by the slope:

$$X_b = h_b/0.05 = 153.6 \text{ ft}$$

By a similar method, the distance of the seawall location from the point of wave breaking can be obtained as follows:

The distance of the seawall from the msl/beach profile intersection is found by dividing the depth at the toe of the wall by the beach slope:

$$= 2.0 \text{ ft}/0.05 = 40.0 \text{ ft}$$

Now,

$$X = X_b - 40.0 = 153.6 - 40.0 = 113.6 \text{ ft}$$

Therefore,

$$X_s = 113.6/153.6 = 0.74.$$

Substituting into Equation 56 yields

$$\begin{aligned} \frac{S_{\max}}{H_b} &= 1.60 (1 - 0.74)^{2/5} \\ &= 0.93 \end{aligned}$$

so that the maximum scoured depth is $S_{\max} = 0.93 (H_b) = 7.1 \text{ ft}$.

39. Using small-scale two-dimensional laboratory studies, Song and Schiller (1973) produced a regression model that predicts relative ultimate scour depth expressed as S_{\max}/H_o . The relative ultimate scour was given as a

function of relative seawall distance X_s and deepwater standing wave steepness H_s/L_s :

$$\frac{S_{\max}}{H_o} = 1.94 + 0.57 \ln(X_s) + 0.72 \ln(H_s/L_s) \quad (53)$$

One problem with this method is the potential for significant differences between standing wave heights and deepwater progressive wave heights. For the condition of unbroken waves impacting the seawall, the SPM (1984) indicates that the maximum H_s can potentially be as high as $2H_o$. For the condition of wave breaking prior to impacting the seawall, the difference between H_s and H_o is less significant and approaches zero when much of the incident wave energy is lost to breaking.

Example 3: For the following given initial design conditions, calculate maximum scour depth.

$$\begin{aligned} d_s &= 0.25 \text{ mm} = 0.00082 \text{ ft} \\ m &= \text{beach slope in front of seawall} = 1:20 \\ H_o &= 6.0 \text{ ft} \\ T_o &= 7 \text{ sec} \\ h_w &= \text{depth at base of wall} = 2.0 \text{ ft} \end{aligned}$$

Solution: Since initial conditions are similar to those in Example 2, the depth of wave breaking is 7.68 ft. This indicates that deepwater parameters can probably be used in Equation 53. X_s was calculated in the previous example and equals 0.74. The next step is to obtain the deepwater standing wave steepness as

$$\begin{aligned} \frac{H_o}{L_o} &= \frac{6.0}{L_o} \\ &= \frac{6.0}{5.12 T^2} \\ &= \frac{6.0}{5.12 (7.0)^2} \\ &= 0.0239 \end{aligned}$$

Substituting into Equation 53 yields

$$\begin{aligned} \frac{S_{\max}}{H_o} &= 1.94 + 0.57 \ln(0.74) + 0.72 \ln(0.0238) \\ &= -0.9234 \end{aligned}$$

so that the maximum scoured depth would be

$$S_{\max} = -5.5 \text{ ft.}$$

The negative value obtained here is due to the sign convention used by Song and Schiller and actually indicates 5.5 ft of scoured sediment.

40. In a study performed at CERC during 1991 and 1992, scaled physical model tests were conducted by Fowler (1992) to investigate toe scour in front of a vertical wall. Twenty-two tests were run for various wave conditions and different wall locations relative to the intersection of msl and the pre-scour beach profile. A statistical analysis of the irregular wave results obtained from this study indicates that ultimate scour depth is most correlated to incident deepwater significant wave height, deepwater wave length, and pre-scour water depth at the wall d_w . Since only one grain size and one initial beach slope were used in the tests, no conclusions were drawn regarding effects of grain size (fall speed) or initial beach slope. However, it can be argued that for the case of a vertical wall with nearly perfect reflection characteristics, the effects of beach slope and reflections are accounted for by the presence of h_w , H_o , and L_o in the equation. Subject to the constraints shown below, the following equation for prediction of maximum depth of scour is proposed based on a mathematical analysis of the irregular wave data:

$$\frac{S_{\max}}{H_o} = \sqrt{22.72 \frac{h_w}{L_o} + 0.25} \quad (54)$$

Use of Equation 54 is limited to cases where $-0.011 \leq h_w/L_o \leq 0.045$ and $0.015 \leq H_o/L_o \leq 0.040$. The last condition restricts the equation to use with waves which are typical of most storms. Maximum scour depths predicted by this equation are plotted versus the measured values from the irregular wave tests in Figure 15.

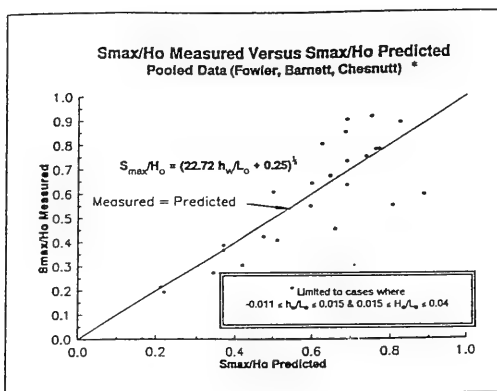


Figure 15. Predicted scour depths versus measured scour depths using proposed equation with irregular wave data only

Example 4: For the following given initial design conditions, calculate maximum scour depth.

$$\begin{aligned}
 d_g &= 0.25 \text{ mm} = 0.00082 \text{ ft} \\
 m &= \text{beach slope in front of seawall} = 1:20 \\
 H_o &= 6.0 \text{ ft} \\
 T_o &= 7 \text{ sec} \\
 h_w &= \text{depth at base of wall} = 2.0 \text{ ft}
 \end{aligned}$$

Solution: The first step is to determine h_w/L_o and H_o/L_o :

$$\begin{aligned}
 \frac{h_w}{L_o} &= \frac{2.0}{250.88} = 0.008 \\
 \text{and} \\
 \frac{H_o}{L_o} &= \frac{6.0}{250.88} = 0.024
 \end{aligned}$$

Since these values fall within the limits of $-0.011 \leq h_w/L_o \leq 0.045$ and $0.015 \leq H_o/L_o \leq 0.040$, Equation 53 may be used to calculate S_{\max} as:

$$\begin{aligned}
 \frac{S_{\max}}{H_o} &= \sqrt{((22.72 \cdot 2.0)/250.88) + .25} \\
 &= 0.66
 \end{aligned}$$

and therefore

$$S_{\max} = 3.94 \text{ ft}$$

41. The following equation was developed by Herbich and Ko (1968) using limited 2-D laboratory data to predict ultimate depth of scour S_{\max} for an initially flat slope where waves do not break prior to impacting the structure:

$$S_{\max} = (h - a_{ir}/2) \left((1 - K_r) u_* \left[3/4 C_D \rho \frac{\cot \phi}{d_g (\gamma_s - \gamma)} \right]^{1/2} - 1 \right) \quad (55)$$

In the above,

$$a_{ir} = H_i + H_r \quad (56)$$

$$K_r = \frac{H_r}{H_i} \quad (57)$$

The above method requires knowledge of a relationship between incident and reflected wave heights, either through measurements made in the laboratory or when available, through published values of K_r . Although Equation 55 was claimed to be in reasonable agreement with results from laboratory model

tests, little effort was made to verify its use in field or larger scale applications. An additional concern is that the equation yields decreasing scour depths with increasing values of K_r . This is directly in contrast to results obtained by other researchers, including Herbich et al. (1984), Chesnutt and Schiller (1971), and Xie (1981). Because of these limitations and apparent discrepancies, Equation 55 is not recommended for use in field applications.

Other Laboratory Studies to Investigate Scour at Seawalls

42. Sato, Tanaka, and Irie (1968) studied scour in front of seawalls for both normal and storm beach profiles. In their study, seawall inclination (angle face of seawall makes with horizontal), grain size, beach slope, and wave conditions were varied using monochromatic waves in a 2-D facility. They identified five different types (modes) of scour described below as:

- Type 1 - Rapid initial scour followed by a gradual accretion of material
- Type 2 - Rapid initial scour leading to beach stability
- Type 3 - Rapid initial scour giving way to slower, but more prolonged erosion
- Type 4 - Continuous gentle scour
- Type 5 - Continuous gentle accretion

In addition to identifying the different scour modes, they reached the following conclusions:

- a. Relative scour depth (S_d/H_o) can be larger than unity for flatter (non-storm) waves, but for storm waves with steepness between 0.02 and 0.04, the relative scour depth was equal to unity.
- b. Relative scour depth decreased with decreasing relative median grain size, (d_{50}/H_o).
- c. Maximum scour depth for storm waves occurred when the wall was located at either the shoreline or just landward of the plunge point.
- d. Maximum scour depths occurred for the Type 3 classification of scour, which is characterized by rapid initial scouring that gives way to slower, more prolonged erosion.
- e. Maximum scour depths occurred for seawall inclinations of 90 deg (vertical) and initial beach slope had little effect for the range of conditions tested.

43. Chesnutt and Schiller (1971) conducted approximately 50 tests in two different wave flumes to investigate scour in front of seawalls along the Texas Gulf Coast. The sand used in their study was Texas beach sand having a

mean diameter of 0.17 mm. The study investigated scour depths associated with various wave conditions, beach slope, seawall locations, and seawall inclination. The more significant findings of this study included:

- a. Maximum scour is approximately equal to the deepwater wave height for the range of conditions tested. Wave steepnesses ranging from 0.003 to 0.036 were run for the cases where the seawall was at a 90-deg (vertical) inclination.
- b. Maximum scour for seawall location occurs in the range of $0.5 < X_s < 0.67$, with X_s as previously defined.
- c. Maximum scour depth increases with an increase in wave height.
- d. Maximum scour depth decreases with a decrease in the angle of inclination of the seawall, or a decrease in the angle the face of the seawall makes with the horizontal.
- e. Maximum scour depth decreases with a decrease in beach slope.

Field Studies

44. Sato, Tanaka, and Irie (1968) also presented field data obtained following a storm which significantly scoured foundations fronting the seawalls at the Port of Kashima. These data supported the findings listed in paragraph 42, particularly the finding that maximum scour depth, S_{max} , is less than or equal to the deepwater significant wave height H_{so} . The measured scour depths at seawalls showed that maximum scour depth under storm conditions was nearly equal to the maximum significant deepwater wave height H_{so} observed during the storm.

45. Sawaragi and Kawasaki (1960) compiled field data on erosion in front of seawalls at eight sites in the Sea of Japan. The data obtained covered a period during which the seawalls were impacted by three significant storms. Analysis of the data led to the conclusion that the maximum depth of scour is approximately equal to the wave height in deep water, and that the location of maximum scour is related (proportional) to the location of the point of breaking of incident waves.

46. Sexton and Moslow (1981) obtained data along seawall-backed beaches at Seabrook Island, South Carolina to examine scour and subsequent recovery following the September 1979 attack of Hurricane David. The beach in front of one concrete seawall experienced a scour depth of 2.1 ft and overtopping also caused some scour on the landward side of the seawall. Since maximum deep-water wave heights exceeded this value considerably, the $S_d/H_0 \leq 1.0$ rule of thumb is apparently supported here as well.

47. Walton and Sensabaugh (1979) examined field data associated with scour which was observed in Panama City, Florida following Hurricane Eloise in September 1975. From their observations, it was noted "that "apparent" seawall scour observed at Panama City ... was considerably less than the maximum predicted by the rule of thumb." Additionally, the authors stated that "most seawalls with cap elevations less than 10 ft above grade" experienced a maximum of 2-3 ft of scour." This observation was for unprotected beaches which fronted seawalls in the area studied.

Scour Prediction at Submerged Pipelines

48. Another situation where scour presents a design problem for coastal engineers and oceanographers is the case of scour around submerged pipelines. For additional discussion of this problem, the reader is referred to Chao and Hennessy (1972), Herbich et al. (1984), and Hales (1980). Chao and Hennessy developed a method for estimating order of magnitude maximum scour depth under offshore pipelines. The method is based primarily on 2-D flow theory and makes use of certain reasonable assumptions, including infinite pipe length, and scour occurring when the velocity in the scour hole is greater than the free stream velocity. Refer to Figure 16 for identification of symbols and

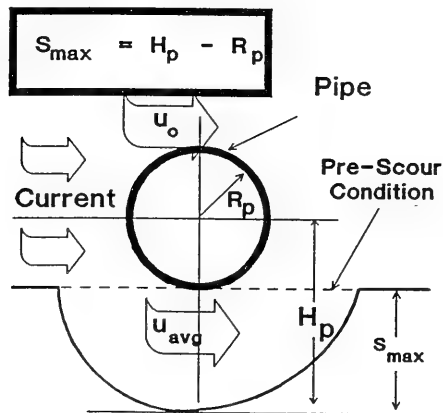


Figure 16. Pipeline scour problem as described by Hennessy and Chao

variables used in the method. Chao and Hennessy's method involves use of the following equations:

$$q_s = u_o \left(H_p - \frac{R_p^2}{2H_p - R_p} \right) \quad \text{for } H_p \geq R_p \quad (58)$$

$$\frac{q_s}{(H_p - R_p)} = u_o \left(\frac{2(H_p/R_p)^2 - (H_p/R_p) - 1}{2(H_p/R_p)^2 - 3(H_p/R_p) + 1} \right) \quad \text{for } H_p \geq R_p \quad (59)$$

$$\tau_b = \frac{f_f \rho (u_{avg})^2}{8} \quad (60)$$

In the above, q_s is the discharge through the scour hole in ft^3/sec , and u_{avg} is the average current velocity in the flow field. Figure 17 is a plot of the friction factor versus Reynolds number R defined as shown in the figure, which allows determination of f_f , the friction factor. In the figure, the roughness factor is defined as

$$\text{Roughness factor} = \frac{R_h}{d_g} \times 10^{-2} \quad (61)$$

with R_h the hydraulic radius, approximated by $H_p - R_p$ (see Figure 16).

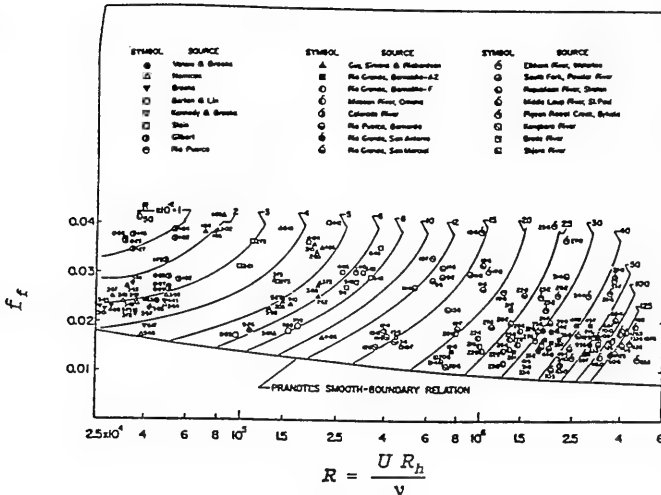


Figure 17. Friction factor versus grain Reynolds number

Using this method, Herbich (1981) has developed a series of charts which can be used to estimate bottom scour for various combinations of sediment size, bottom current velocity, and pipeline diameter. Similar calculations have been performed to produce Figure 18 below, which is typical of those found in Herbich (1981). Use of this figure is illustrated in example 5 below.

Example 5. For the following given initial design conditions, calculate maximum pipeline scour depth.

- d_g = 0.0082 ft
- H_o = 6.0 ft
- T_o = 7.0 sec
- R_p = 1.0 ft = pipe outside radius
- u_o = current velocity at top of pipeline,
2.0 ft/sec based on field measurements

Solution: Simply enter Figure 18 on the horizontal axis at $u_o = 2.0$ ft and locate the curve for the 24-in. outside diameter. Then read maximum scour depth, S_{max} , from the vertical axis to be 2.5 ft.

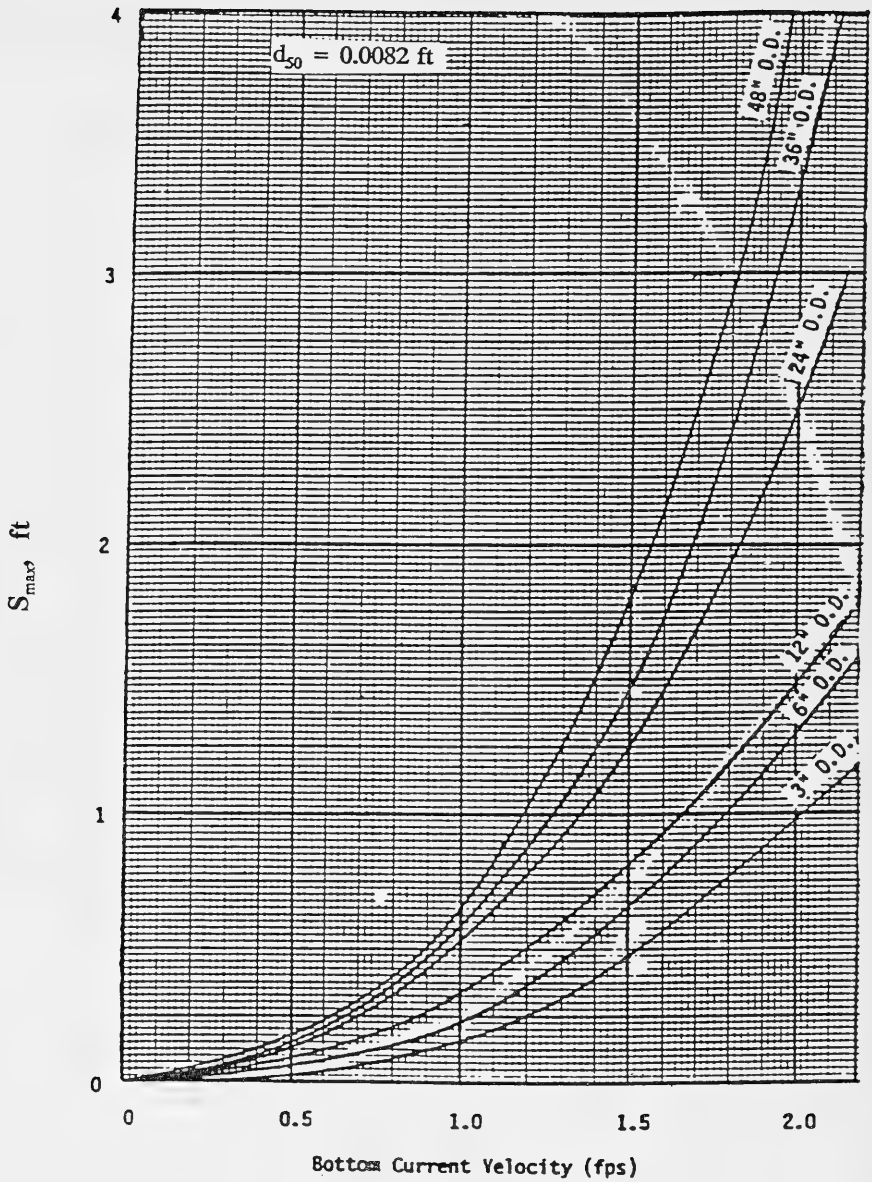


Figure 18. Maximum pipeline scour as a function of bottom velocity for $d_g = 0.0082 \text{ ft}$

PART V: MODELING SCOUR AT COASTAL STRUCTURES
USING MOVABLE-BED PHYSICAL MODELS

General

49. The following sections provide a brief discussion of physical hydraulic modeling as abstracted from Fowler and Smith (1986).

Model and Prototype Similarities

50. When conducting scaled physical model tests of prototype phenomena, for exact reproduction, three types of similarity are required between model and prototype (i.e., the model and prototype must be geometrically, kinematically, and dynamically similar). Without similarity, results from the model tests cannot be extrapolated to render meaningful prototype results.

51. For geometric similarity, the ratio of model-to-prototype lengths must be the same for all corresponding lengths. Dynamic similarity is achieved when all relevant forces which act on corresponding masses in the model and prototype occur in the same ratio ($F_p/F_m = \text{constant}$) throughout the flow fields. For precise modeling of any fluid prototype, ratios of all of the above forces must be equivalent in model and prototype. Short of modeling at a 1:1 (prototype) scale, no fluid exists with viscosity, surface tension, and elasticity that will satisfy this equivalency requirement. Fortunately, only one or two of these forces are dominant in a given phenomenon and the other forces may be neglected with little error. For coastal modeling studies, inertia and gravity forces are dominant and Froude scaling guidelines are used for hydraulic parameters. Also, since turbulent flow exists in most prototype situations, the scale is selected such that the model Reynolds number, $R = \rho U l / \mu$, where U , the average velocity, is greater than the critical Reynolds number (so that turbulent flow is obtained). Kinematic similarity requires that fluid flow patterns in model and prototype be similar. If all force ratios and geometric length ratios are similar in model and prototype, kinematic similarity is ensured.

Movable-Bed Modeling Guidance

52. In general, most researchers agree that two approaches/concepts are important in modeling how particles are moved from one bed location to another:

- a. Fall velocity similarity.
- b. Incipient motion similarity.

Recent studies (Hughes and Fowler 1990) indicate that the fall speed scaling guidance produces good results for energetic situations such as occur in the surf zone where turbulent energy associated with breaking waves dominates. Scaling by incipient motion criteria is more appropriate in situations where sediment transport is predominantly by bed load. Since the overwhelming majority of sediment transport for these tests was by suspended load, the fall speed guidance was used. Appropriate fall speed scaling criteria are:

Fall Speed Scaling Guidance for Wave-Energy-Dominated Erosion

- 1) Fall speed parameter ($H/\omega T$) similarity.
- 2) Time scaled by Froude ($Fr = V/(g\ell)^{1/2}$) similarity.
- 3) Model is undistorted ($N_t = N_x = N_y = N_z$).
- 4) Use fine sand ($d_s = 0.08\text{mm}$ lower limit) as model sediment at largest possible scale ratio.

For the above items:

- V = an appropriate velocity
- ℓ = characteristic length
- N = scale ratio (prototype to model)

Subscripts ℓ , x , y , and z are characteristic length, length in the x direction, length in the y direction, and length in the z direction, respectively. Similarity between model and prototype fall speed parameters is achieved when

$$\left[\frac{H}{\omega T} \right]_{model} = \left[\frac{H}{\omega T} \right]_{prototype} \quad (62)$$

which, for an undistorted model, reduces to

$$N_{\omega} = \sqrt{N} \quad (63)$$

For the above, N_{ω} is the prototype-to-model fall speed ratio and N_t is the prototype-to-model length scale ratio. The Froude scaling guidance is given by

$$N_t = \sqrt{N} \quad (64)$$

where N_t is the prototype-to-model time scale ratio. Equations 62, 63, and 64 can be combined to yield a unique scaling guidance that satisfies the first two scaling criteria:

$$N_{\omega} = \sqrt{N} = N_t \quad (65)$$

Recent Successes with Movable-Bed Model Studies

53. During the past several years at CERC numerous studies concerning various problems associated with physical movable-bed models have led to very important findings. The successes of the most recent accomplishments will allow engineers and scientists to use these models as a tool for planning and designing various coastal projects where storm-induced erosion is a major consideration. This is particularly important because the methods and procedures for movable-bed models are not widely accepted and numerous (often conflicting) guidances have been developed. A scaled physical model was recently used to validate the above guidance by simulating prototype scale wave-induced scour in front of a concrete dike sloped at 1:4. The tests were conducted during fall and winter of 1988. Prototype data used were obtained from the large wave tank tests done by Dette and Uliczka (1987) at the University of Hannover in Germany during 1985 and 1986. Based on the very successful results of this study, the modeling guidance was considered validated for the stated conditions. Following the validation tests, the scaling guidance was used to simulate severe beach fill erosion associated with a winter storm at Ocean City, Maryland during March 1989. The tests were conducted without prior knowledge of post-storm profiles and results indicated that model and prototype profiles showed good agreement, giving further credence to the scaling guidance and its ability to model energetic (erosive) wave-action movable-bed situations. In addition to the above, the studies by Fowler (1992) referenced in paragraph 40 also successfully used the fall speed guidance for movable-bed studies on scour in front of vertical seawalls.

PART VI: SUMMARY

54. It may well be unreasonable to expect that a single scour prediction method will yield consistent and reliable results for all cases. This report has briefly discussed the merits and shortcomings of the several scour prediction techniques for various coastal scour situations. In general, prediction techniques for scour at structure toes are either rule-of-thumb methods or semi-empirical equations based on limited laboratory and field studies. Table 2 contains recommended methods for estimating maximum scour depths for inclusion in coastal structure designs. Probably sufficient guidance exists for vertical walls, piles, and pipelines. Additional research is needed in the area of rubble-mound structure scour prediction methods.

Rubble-Mound Structures

55. Very little guidance is available for prediction of scour depths at the base of rubble-mound structures. This is not due to a lack of laboratory or field study efforts - basically, the magnitude of the scour is difficult to measure directly since the structure typically collapses onto itself and fills the holes. In addition to research efforts associated with scour at rubble-mound structures being conducted as a part of the "Laboratory Studies on Scour" work unit, a three-dimensional scaled laboratory model study entitled "Scour Holes at the Ends of Structures" under the U.S. Army Corps of Engineers, Coastal R & D Program, is being conducted to gain understanding of processes that occur during formation of scour holes at structures. The majority of efforts in this area have focused on predicting the size and amount of toe protection which should be used to avoid significant damage to the structures. Usually, general guidelines based on laboratory and field studies are used to design jetties, breakwaters, and revetments which have varying degrees of toe scour protection. Hales (1980) conducted a survey of scour protection practices in the United States and found that a rule of thumb for minimum toe scour protection is a toe apron measuring 2.0 to 3.28 ft thick and 4.9 ft wide. Eckert (1983) subsequently found that toe scour protection should be designed to accommodate the maximum scouring force that exists where wave downrush on the structure face extends to the toe. According to Eckert, the rule of thumb for minimum toe scour protection suggested by Hales will be inadequate under certain conditions (see section IV) involving water depth and wave reflection.

56. Laboratory model studies by Markle (1989) produced the most recent guidance for sizing toe berm armor stone and toe buttressing stone. Guidance is given in terms of the stability number N_s , as defined in paragraph 33

Table 2
Scour Prediction Methods For Various Scour Modes

Scour Mode	Recommended Method	Appropriate Equation(s)	Remarks
Vertical Piles	Herbich et al (1984)	$\log_{10}\left(\frac{S_L}{h}\right) = -1.2935 + 0.1917 \log_{10}\beta$ $\log_{10}\left(\frac{S_E}{h}\right) = -1.4071 + 0.2667 \log_{10}\beta$	Provides method for estimating local and general scour
Submerged Pipelines	Chao and Hennessy(1972)	$q_s = u_o \left(H_p - \frac{R_p^2}{2H_p - R_p} \right)$ $\frac{q_s}{(H_p - R_p)} = u_o \left(\frac{2(H_p/R_p)^2 - (H_p/R_p) - 1}{2(H_p/R_p)^2 - 3(H_p/R_p) + 1} \right)$	Provides order of magnitude estimates only
Vertical Seawalls	SPM (1984)	$S_{max}/H_o \leq 1$	Some laboratory data using regular waves have exceeded this rule
Vertical Seawalls	Fowler (1992)	$\frac{S_{max}}{H_o} = \sqrt{22.72 h_w/L_o + .25}$	Valid for cases where $-0.011 \leq h_w/L_o \leq 0.05$ and $0.015 \leq H_o \leq 0.04$
Smaller Rubble Mound Structures in Shallow Water	Rule of thumb	$S_{max}/H_o \leq 1$	This has not been proven for rubble-mound structures, but should be sufficient for revetments and shallow-water rubble-mound groins
Rubble-Mound Structures in Deep Water	Markle (1989)	Stability number guidance is given for toe berm and toe buttressing stone design for wave stability only.	No guidance for scour depth estimation or protection is yet available

for toe berm stone stability against wave action (not scour protection). The guidance states that "unless site-specific model tests are conducted to justify higher values of N_s , stability number should be selected based on the lower limit curves presented in Figures 11 and 12, and the individual toe berm armor stone weights should range from a maximum of $1.3 W_{50}$ to a minimum of $0.7 W_{50}$." For toe buttressing stone protection for wave stability only, limited 2-D stability tests for toe buttressing a one-layer uniformly placed tri-bar structure, a stability number N_s equal to 1.5 should be used in a wave-breaking environment.

57. For smaller rubble-mound structures such as revetments, the $S_{\max}/H_o \leq 1$ rule of thumb, which was developed for use with vertical seawalls, should be appropriate for determining ultimate scour depth. In such cases, structures should be designed such that the seaward face of the structure is extended downward to the expected scour depth, typically equal to the maximum wave height carried in that depth of water.

Vertical Piles and Similar Structures

58. For scour prediction methods at vertical piles, the method discussed in Section IV by Herbich et al. (1984) should provide sufficient design guidance.

Vertical Wall Structures

59. Results from Fowler (1992) and numerous field studies tend to support the widely used rule of thumb which states that $S_{\max}/H_o \leq 1$. Another rule-of-thumb method, Dean's approximate principle, appears to be supported by numerous laboratory studies and limited field observations; however, a major shortcoming of this method is that it requires determination of beach profiles for given sediments and wave climate both prior to and subsequent to a design event. At present, this is quite difficult to accomplish. When used with various semi-empirical equations for prediction of S_{\max} , the equation of Song and Schiller (1973) performed reasonably well within the limits of applicability given by $0.5 \leq X/X_b \leq 1$. An empirical equation based solely on irregular laboratory wave data also has been proposed subject to previously described limitations and appears to predict scour depth observed by others quite well (Chesnutt and Schiller 1971, Barnett 1987).

60. For seawalls constructed in areas where $-0.011 \leq h_w/L_o \leq 0.05$ and $0.015 \leq H_o \leq 0.04$,

$$\frac{S_{\max}}{H_o} = \sqrt{22.72 h_w/L_o + 0.25} \quad (66)$$

is recommended for determining ultimate scour depth. For all other cases, the $S_{\max}/H_o \leq 1$ rule of thumb should be appropriate for determining ultimate scour depth at vertical walls.

Submerged Pipelines

61. The method developed by Chao and Hennessy (1972) for estimating order of magnitude maximum scour depth under offshore pipelines is fairly straightforward and should provide reasonable predictions. Herbich (1981) used Chao and Hennessy's method to develop a series of charts that can be conveniently used to estimate bottom scour for various combinations of sediment size, bottom current velocity, and pipeline diameter.

REFERENCES

- Abou-Seida, M. M. 1964 (September). "Sediment Scour at Structures," Technical Report HEL-4-2, University of California, Hydraulic Engineering Laboratory, Wave Research Projects, Berkeley, CA.
- _____. 1965. "Bed Load Function Due to Wave Action," Technical Report HEL-2-11, University of California, Berkeley, CA.
- Athow, Robert F., and Pankow, Walter E. 1986 (July). "Annotated Bibliography for Navigation Training Structures," Technical Report REMR-HY-1, US Army Engineer Waterways Experiment Station, Estuaries Division, Hydraulics Laboratory, Vicksburg, MS.
- Barnett, M. R. 1987. "Laboratory Study of the Effects of a Vertical Seawall on Beach Profile Response," Report 87/005, Coastal and Oceanographic Engineering Department, University of Florida, Gainesville, FL.
- Brebner, A., and Donnelly, P. 1962. "Laboratory Study of Rubble Foundations for Vertical Breakwaters," Civil Engineering Research Report No. 23, Queens University, Kingston, Ontario.
- Carpenter, L. H., and Keulegan, Garbis H. 1958. "Forces on Cylinders and Plates in an Oscillating Fluid," J. Res. National Bur. Standards, Vol 60, No. 5, pp 423-440.
- Chao, J. L., and Hennessy, P. V. 1972. "Local Scour Under Ocean-Outfall Pipelines," Journal of Water Pollution Control Fed., Vol 44, No. 7, pp 1443-1447.
- Chesnutt, C. B., and Schiller, R. E., Jr. 1971. "Scour of Simulated Gulf Coast Sand Beaches Due to Wave Action in Front of Sea Walls and Dune Barriers," Sea Grant Publication No. 71-207, Texas A&M University, College Station, TX.
- Clark, Douglas F. 1979. "Prediction of the Initiation of Motion of Organic Sediments on Sand and Gravel Beds," M. S. thesis, Clemson University, Clemson, SC.
- Dean, R. G. 1986. Coastal Armoring: Effects, Principles and Mitigation," Proceedings of the 20th Coastal Engineering Conference, American Society of Civil Engineers, Vol 3, pp 1843-1857.
- Dette, H. H., and Uliczka, K. 1987. Prototype Investigation on Time-Dependent Dune Recession and Beach Erosion," Proceedings of Coastal Sediments '87, American Society of Civil Engineers, Vol 2, pp 1430-1444.
- DuBoys, P. 1879. "Le Rhone et les Riviers a lit Affonillable (French) (The Rhone and Streams with Movable Beds)," Annals des Pontes et Chaussees, Ser. 5, Tome (Vol) XVIII, pp 141-195.
- Eagleson, P. S., and Dean, R. G. 1966. "Small Amplitude Wave Theory," Estuary and Coastline Hydrodynamics, A. T. Ippen, ed., McGraw-Hill, Inc., NY, pp 1-92.
- Eckert, J. W. 1983. "Design of Toe Protection for Coastal Structures," Proceedings of Coastal Structures '83, American Society of Civil Engineers, Alexandria, VA, pp 331-341.
- Einstein, H. A. 1950 (September). "The Bed-load Function for Sediment Transportation in Open Channel Flows," US Soil Conservation Service Technical Bulletin No. 1026, United States Department of Agriculture.

- Einstein, H. A., and Wiegel, R. L. 1970 (Feb). "A Literature Review on Erosion and Deposition of Sediment Near Structures in the Ocean (U)," Final Report HEL-21-6, US Naval Civil Engineering Laboratory, Port Hueneme, CA.
- Fowler, J. E. 1992. "Scour Problems and Methods for Prediction of Maximum Scour at Vertical Seawalls," Technical Report CERC 92-16, US Army Engineer Waterways Experiment Station, Coastal Engineering Research Center, Vicksburg, MS.
- Fowler, J. E., and Smith, E. R. 1986. "Evaluation of Movable-Bed Modeling Guidance," Proceedings, Third International Symposium on River Sedimentation, S. Wang, H. Shen, and L. Ding, eds., University of Mississippi, pp 1793-1802.
- Fowler, J. E., and Hughes, S. A. 1989. "Mid-Scale Laboratory Tests on Two-Dimensional Movable Bed Sand Model," Proceedings, Third International Symposium on Sediment Transport Modeling, American Society of Civil Engineers, pp 332-337.
- Goda, Y. 1970. "A Synthesis of Breaker Indices," Transactions of the Japanese Society of Civil Engineers, Vol 2, Pt.2.
- Hales, Lyndall Z. 1980. "Erosion Control of Scour During Construction; Report 2, Literature Survey of Theoretical, Experimental and Prototype Investigations," Technical Report HL-80-3, US Army Engineer Waterways Experiment Station, Vicksburg, MS.
- Hallermeier, R. J. 1981 (Jul). "Critical Wave Conditions for Sand Motion Initiation," CETA 81-10, Department of the Army, Coastal Engineering Research Center, Fort Belvoir, VA.
- Herbich, J. B., and Ko, S. C. 1968. "Scour of Sand Beaches in Front of Seawalls," Proceedings of the Eleventh Conference on Coastal Engineering, pp 622-643.
- Herbich, John B. 1981. "Offshore Pipeline Design Elements," Marine Technology Society.
- Herbich, John B., Schiller, Robert E., Jr., Dunlap, Wayne A. and Watanabe, Ronald K. 1984. "Seafloor Scour; Design Guidelines for Ocean-Founded Structures," Marine Technology Society.
- Hudson, R. Y. 1961. "Laboratory Investigation of Rubble-Mound Breakwaters," Transactions of the American Society of Civil Engineers, American Society Civil Engineers, Vol 126, Pt. IV.
- Hughes, S. A., and Fowler, J. E. 1990. "Mid-Scale Physical Model Validation for Scour at Coastal Structures," Technical Report CERC 90-8, US Army Engineer Waterways Experiment Station, Coastal Engineering Research Center, Vicksburg, MS.
- Ishihara, T., and Sawaragi, T. 1962. "Laboratory Studies on Sand Drift, the Critical Velocity and the Critical Water Depth for Sand Movement, and the Rate of Transport Under Wave Action," Fundamental Studies on Dynamics of Sand Drifts, Coastal Engineering in Japan, Report 3, Vol 5, pp 59-65.
- Jones, D. F. 1975. "The Effect of Vertical Seawalls on Longshore Currents," Ph.D. dissertation, University of Florida.
- Kalinske, A. A. 1947 (Aug). "Movement of Sediment as Bed Load in Rivers," Transactions of the American Geophysical Union, Vol 28, p 615.
- Kalkanis, G. 1963. "Transportation of Bed Material Due to Wave Action," Technical Report HEL-2-4, University of California, Berkeley, CA.
- Kana, T. W. 1978. "Surf Zone Measurements of Suspended Sediment," Proceedings, Sixteenth Coastal Engineering Conference, Hamburg, Germany, Vol II, pp 1725-1743.

- Komar, P. D., and Miller, M. C. 1974. "Sediment Threshold Under Oscillatory Waves," Proceedings, Fourteenth Coastal Engineering Conference, Copenhagen, Denmark, pp 756-775.
- Kraus, N. C. 1988. "The Effects of Seawalls on the Beach: An Extended Literature Review," Journal of Coastal Research, Special Issue No. 4, N. C. Kraus and O. H. Pilkey, eds., pp 1-28.
- Kurihara, M., Shinohara, K., Tsubaki, T., and Yoshioka, M. 1956. "Coastal Sediment Movement Due to Wave Action," Proceedings of the Third Conference on Coastal Engineering in Japan, pp 151-162.
- Lane, E. W., and Kalinske, A. A. 1941. "Engineering Calculations of Suspended Sediment," Transactions, American Geophysical Union, Vol 22, pp 603-607.
- Larson, M., and Kraus, N. C. 1989. "SBEACH: Numerical Model for Simulating Storm-Induced Beach Change; Report 1, Empirical Foundation and Model Development," Technical Report CERC-89-9, US Army Engineer Waterways Experiment Station, Coastal Engineering Research Center, Vicksburg, MS.
- Lee, T. T. 1970 (Sept). "Estuary Inlet Channel Stabilization Study Using a Hydraulic Model," Proceedings of the Twelfth Coastal Engineering Conference, American Society of Civil Engineers, Washington, D.C., pp 1117-1136.
- _____. 1972 (Jul). "Design of Filter System for Rubble-Mound Structures," Proceedings of the Thirteenth Coastal Engineering Conference, American Society of Civil Engineers, Vancouver, B.C., Canada, pp 1917-1933.
- MacDonald, T. C. 1973. "Sediment Transport Due to Oscillatory Waves," Technical Report HEL-2-39, University of California, Berkeley, CA.
- Madsen, O. S., and Grant, W. D. 1975. "The Threshold of Sediment Movement Under Oscillatory Waves: A Discussion," Journal of Sedimentary Petrology, Vol 45, pp 360-361.
- _____. 1976. "Quantitative Description of Sediment Transport by Waves," Proceedings, Fifteenth Coastal Engineering Conference, Honolulu, Hawaii, Part II, pp 1093-1112.
- Markle, Dennis G. 1986 (Dec). "Stability of Rubble-Mound Breakwater and Jetty Toes: Survey of Field Experience," Technical Report REMR-CO-1, US Army Engineer Waterways Experiment Station, Vicksburg, MS.
- _____. 1989. "Stability of Toe Berm Armor Stone and Toe Butressing Stone on Rubble-Mound Breakwaters and Jetties," Technical Report REMR-CO-12, US Army Engineer Waterways Experiment Station, Vicksburg, MS.
- Middleton, G. V., and Southard, J. B. 1977. "Mechanics of Sediment Movement," Lecture Notes for Short Course No. 3, Eastern Section of SEPM, Binghamton, New York, March 29-30, 1977.
- Pilarczyk, K. W. 1989. "Short Course on Design of Coastal Structures: Dimensioning Aspects of Coastal Protection Structures Dikes And Revetments," Delft, The Netherlands.
- Powell, K. A. 1987. "Toe Scour at Sea Walls Subject to Wave Action," Report SR 119, Hydraulic Research Limited, Wallingford, UK.
- Rouse, H. 1938. "Transportation of Sediment," Fluid Mechanics for Hydraulic Engineers, McGraw-Hill, New York.
- _____. 1939. "Experiments on the Mechanics of Sediment Suspension," Proceedings of the International Congress of Applied Mechanics, 5th Congress, Cambridge, pp. 550-554.

- Sato, S., Tanaka, N., and Irie, I. 1968. "Study on Scouring at the Foot of Coastal Structures," Proceedings, Eleventh Conference on Coastal Engineering, London, England, Vol I, pp 579-598.
- Sato, S., and Kishi, T. 1954. "Shearing Force on Sea Bed and Movement of Bed Material Due to Wave Motion," J. Res. of Public Works Res. Inst. 1(paper 3): 1-11.
- Sawaragi, T. 1966. "Scouring Due to Wave Action at the Toe of Permeable Coastal Structures," Proceedings, Tenth Conference on Coastal Engineering, Tokyo, Japan, pp 1036-1047.
- Sawaragi, T., and Kawasaki, Y. 1960. "Experimental Study on Behaviours of Scouring at the Toe of Seadikes by Waves," Proceedings of the 4th Japanese Coastal Engineering Conference, Japan Society of Civil Engineers, pp 1-12.
- Sexton, W. J., and Moslow, T. F. 1981. "Effects of Hurricane David, 1979, on the Beaches of Seabrook Island, South Carolina," Northeastern Geology, Vol 3, Nos. 3 and 4, pp 297-305.
- Shields, A. 1936. Anwendung der Ahnlichkeitsmechanik und der Turbulenzforschung auf die Geschiebebewegung: Mitteilungen der Preuss. Versuchsanst. für Wasserbau und Schiffbau, Berlin, vol 26, translated by W. P. Ott and J. C. van Uchelen, US Department of Agriculture, US Soil Conservation Service Coop. Lab., California Institute of Technology.
- Shore Protection Manual. 1984. 4th ed., 2 Vols, US Army Engineer Waterways Experiment Station, Coastal Engineering Research Center, US Government Printing Office, Washington, DC.
- Silvester, R. 1974. "Sedimentation, Estuaries, Tides, Effluents and Modelling," Coastal Engineering II, Department of Civil Engineering, University of Western Australia, Nedlands, W.A., Australia.
- Song, Won Oh, and Schiller, Robert E. 1973 (Jun). "Experimental Studies of Beach Scour," C.O.E. Report No. 166, Texas A&M Sea Grant College.
- Straub, L. G. 1942. "Mechanics of Rivers," Hydrology, Dover, NY.
- Swart, D. H. 1974. "Offshore Sediment Transport and Equilibrium Beach Profiles," Publication No. 131, Delft Hydraulics Laboratory, Delft, The Netherlands.
- Walton, T. L., and Sensabaugh, W. 1979. "Seawall Design on the Open Coast," Sea Grant Report No. 29, State University System of Florida, Sea Grant College Program.
- Xie, S.-L., 1981. "Scouring Patterns in Front of Vertical Breakwaters and Their Influences on the Stability of the Foundations of the Breakwaters," Department of Civil Engineering, Delft University of Technology, The Netherlands.
- Yang, C. T. 1973. "Incipient Motion and Sediment Transport," Journal of the Hydraulics Division, American Society of Civil Engineers, Vol 99, No. HY10.

APPENDIX A: NOTATION

a	Wave amplitude
a_{ir}	Sum of incident and reflected wave heights
A_o	Orbital diameter of wave motion
A_s	Projected area of a sediment grain
B_{apron}	Apron width
C_o	Initial sediment concentration for use in MacDonald's (1973) sediment concentration equation
C_1	"Shape" coefficient
C_2	Drag coefficient
C_A	Known concentration at height A above the bed
C_D	Drag coefficient
C_s	Sediment concentration in the water
d	Arbitrary representative particle diameter, typically mean or median
d_1	Depth from still-water level to top of toe for stable rubble-mound structure using Markle (1989) guidance
d_e	Equivalent effective bottom roughness
d_g	Median grain diameter
d_s	Depth from still-water level to sediment base on which rubble-mound structure resides using Markle (1989) guidance
d_u	Uniform grain size
D	Drag force
D_p	Pile diameter
f_f	Friction factor for use in Prandtl's chart
f_w	Friction factor for wave motion on bottom
Fr	Froude number, $V/(gL)^{1/2}$ or $U/(gL)^{1/2}$
g	Acceleration due to gravity, 32.2 ft/sec ² or 9.8 m/s ²
h	Depth
h_1	Depth used in Sawaragi's equation for breakwaters
h_2	Depth used in Sawaragi's equation for breakwaters
h_b	Depth of water at point of wave breaking
h_c	Critical water depth
h_u	Depth of uniform flow
h_w	Depth of water in front of seawall
H	Wave height
H_o	Deepwater wave height
H_b	Breaking wave height
H_c	Critical wave height
H_D	Design wave height
H_i	Incident wave height
H_p	Vertical distance from center of pipe to maximum scour depth
H_r	Reflected wave height
H_s	Standing wave height
H_{so}	Deepwater significant wave height

k_{Δ}	Layer coefficient varying between 0.94 and 1.15
K_D	Stability coefficient for armor stone equation
K_r	Reflection coefficient
l	Length used in Sawaragi's stable rubble-mound structure cross-section equation
l_r	Ripple length
l	Characteristic length
L	Lift force
L_o	Deepwater wave length
L_s	Standing wave length
l	Characteristic size of structure, ft
m	Beach slope
M	Coefficient for use in MacDonald's (1973) sediment concentration equation
n	Manning's roughness coefficient
n_r	Ripple height
n_s	Number of stones
N	Scale ratio
N_l	Length scale ratio
N_s	Stability number for berm armor stone design
N_t	Time scale ratio
N_x	x length scale ratio
N_y	y length scale ratio
N_z	z length scale ratio
N_w	Sediment fall speed scale ratio
q	Hydraulic discharge rate
q_b	Bed-load transport rate
q_{cr}	Critical sediment transport rate per unit width of channel
q_s	Sediment transport rate per unit width of channel
q_S	Discharge through the scour hole under pipeline
R	Height from sea level to limit of wave runup on Sawaragi structure
R_c	Height of the top of the structure relative to sea level when Sawaragi's structure is overtopped
R	Reynolds number
R_g	Grain Reynolds number
R_p	Pipe radius
R_h	Hydraulic radius
sg	Specific gravity of sediment
s	Slope of face of breakwater section used in Sawaragi equation
s'	Slope of face of breakwater section used in Sawaragi equation
S	Channel slope
S_d	Depth of scour
S_1	Ultimate local scour depth at vertical piles
S_{max}	Maximum depth of scour

S_r	Specific gravity of berm stone relative to the water in which structure resides
S_t	Ultimate total scour depth at vertical piles
SS_{10}	Suspended sediment concentration at 10-cm elevation above bed
SWL	Still-water level
t	Time
T	Wave period
T_o	Deepwater wave period
u	Near-bottom maximum horizontal orbital velocity
u_o	Current velocity at top of pipeline
u_*	Shear velocity = $(\tau/\rho)^{1/2}$
u_{avg}	Average jet velocity through the scoured area under a pipeline
u_b	Near-bottom current velocity
u_{crit}	Orbital near-bottom critical horizontal velocity
u_{max}	Near-bed maximum orbital velocity
U	Average flow velocity
V	Velocity
V_c	Critical velocity
V_s	Volume of a sediment grain
W	Weight of particle
W_a	Mean weight of primary armor stones
W_{apron}	Unit weight of stones to be used in apron for toe protection
W_{50}	Median weight of individual berm stone in lb_f
X	Distance from seawall from the point of wave breaking
X_b	Distance from intersection of beach profile and mean sea level to the point of wave breaking
X_M	Dimensionless variable defined by Madsen and Grant (1976)
X_s	Dimensionless location of seawall relative to intersection of mean sea level and pre-scour beach profile
Y_M	Dimensionless variable defined by Madsen and Grant (1976)
Y	Elevation above the bed
z	Distance above bed

Greek Letter symbols

A	Arbitrary height above bottom
α	Parameter used to parameterize scour at vertical piles
α_{crit}	Empirically obtained coefficient for critical water depth calculation
β	Parameter used to parameterize scour at vertical piles
ρ_s	Density of sediment grains
ρ	Fluid density
ω	Sediment fall speed

ϕ	Angle of sides of scour hole, approximately equal to the angle of repose of the grains
ϕ_s	Angle of repose for a given sediment grain, degrees
θ	Angle of the structure slope measured relative to horizontal plane
Φ	Dimensionless measure of bed-load transport
ψ	Einstein bed-load function
ϵ	Diffusion coefficient
γ	Specific weight of water, either fresh or salt, as appropriate
γ_s	Specific weight of sediment
γ_r	Specific weight of armor unit
γ_{rb}	Specific weight of berm stone, lb_f/ft^3
τ_b	Bed or boundary shear stress
τ_o	Bed or boundary shear stress
τ_c	Critical boundary shear stress to initiate movement
ν	Kinematic viscosity = μ/ρ
μ	Fluid dynamic viscosity
η	Empirically obtained exponent for critical water depth calculations

REPORT DOCUMENTATION PAGE

Form Approved
OMB No. 0704-0188

Public reporting burden for this collection of information is estimated to average 1 hour per response, including the time for reviewing instructions, searching existing data sources, gathering and maintaining the data needed, and completing and reviewing the collection of information. Send comments regarding this burden estimate or any other aspect of this collection of information, including suggestions for reducing this burden, to Washington Headquarters Services, Directorate for Information Operations and Reports, 1215 Jefferson Davis Highway, Suite 1204, Arlington, VA 22202-4302, and to the Office of Management and Budget, Paperwork Reduction Project (0704-0188), Washington, DC 20503.

1. AGENCY USE ONLY (Leave blank)		2. REPORT DATE May 1993	3. REPORT TYPE AND DATES COVERED Final report		
4. TITLE AND SUBTITLE Coastal Scour Problems and Methods for Prediction of Maximum Scour			5. FUNDING NUMBERS		
6. AUTHOR(S) Jimmy E. Fowler					
7. PERFORMING ORGANIZATION NAME(S) AND ADDRESS(ES) U.S. Army Engineer Waterways Experiment Station Coastal Engineering Research Center 3909 Halls Ferry Road, Vicksburg, MS 39180-6199			8. PERFORMING ORGANIZATION REPORT NUMBER Technical Report CERC-93-8		
9. SPONSORING/MONITORING AGENCY NAME(S) AND ADDRESS(ES) U.S. Army Corps of Engineers Washington, DC 20314-1000			10. SPONSORING/MONITORING AGENCY REPORT NUMBER		
11. SUPPLEMENTARY NOTES Available from National Technical Information Service, 5285 Port Royal Road, Springfield, VA 22161.					
12a. DISTRIBUTION/AVAILABILITY STATEMENT Approved for public release; distribution is unlimited.			12b. DISTRIBUTION CODE		
13. ABSTRACT (Maximum 200 words) The most common coastal scour-related problems are toe scour at rubble-mound structures and vertical seawalls, and scour at the base of piles and horizontal pipelines. Existing scour prediction methods for these problems vary from rules of thumb to empirically derived equations to theoretically derived relationships. Recent studies at the U.S. Army Engineer Waterways Experiment Station's Coastal Engineering Research Center indicate that sufficient design guidance exists for vertical walls, pipelines, and vertical piles; however, additional research is still needed for rubble-mound structures.					
14. SUBJECT TERMS Coastal Flume studies Irregular waves			Moveable bed model Physical model Scour	Scour prediction Seawall Sedimentation	15. NUMBER OF PAGES 65
					16. PRICE CODE
17. SECURITY CLASSIFICATION OF REPORT UNCLASSIFIED	18. SECURITY CLASSIFICATION OF THIS PAGE UNCLASSIFIED	19. SECURITY CLASSIFICATION OF ABSTRACT	20. LIMITATION OF ABSTRACT		

Destroy this report when no longer needed. Do not return it to the originator.

DEPARTMENT OF THE ARMY

WATERWAYS EXPERIMENT STATION, CORPS OF ENGINEERS
3909 HALLS FERRY ROAD
VICKSBURG, MISSISSIPPI 39180-6199

Official Business

SPECIAL
FOURTH CLASS
U.S. POSTAGE PAID
VICKSBURG, MS
PERMIT NO. 85

287/L12/ 1
WOODS HOLE OCEANOGRAPHIC INSTITUTION
DOCUMENTS LIBRARY/CLARK 141
WOODS HOLE MA 02543-1098